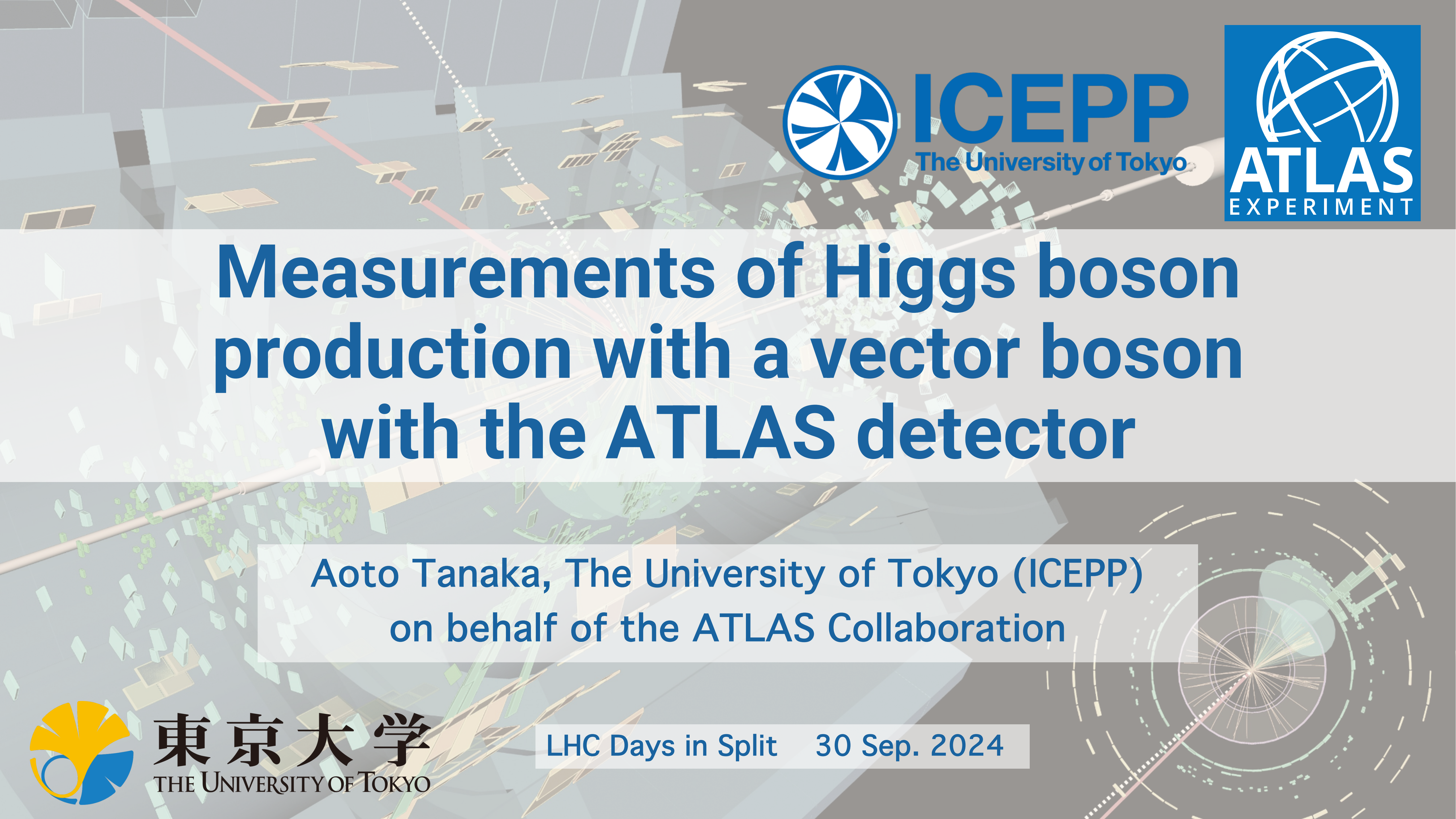

Measurements of Higgs boson production with a vector boson with the ATLAS detector

Aoto Tanaka, The University of Tokyo (ICEPP)
on behalf of the ATLAS Collaboration

LHC Days in Split   30 Sep. 2024

Vector boson associated Higgs (VH) production

- Physics motivation of Higgs precise measurement
  - ➢ Search the deviation from the SM by:
    - ･ Coupling constant of Higgs
    - ･ Fiducial differential cross-section

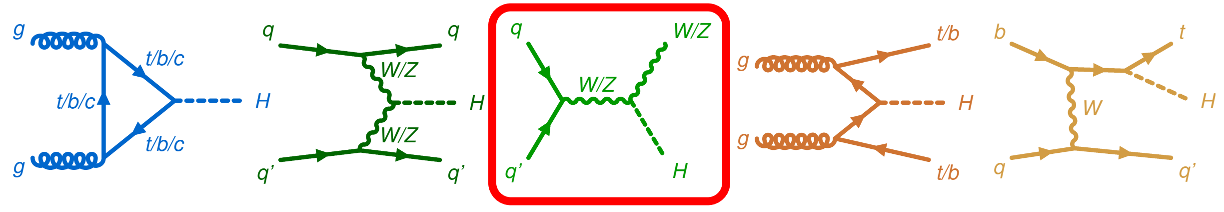

cross-section fraction :

~87 % ~7 % **~4 %** ~1 % ~0.05 %

- Difficulty of VH measurement
  - ➢ Low VH cross-section × branching ratio
    - ･ H → bb channel earns enough statistic
  - → Need to constrain huge background

[*Nature* **volume 607**, pages 52–59 (2022)]

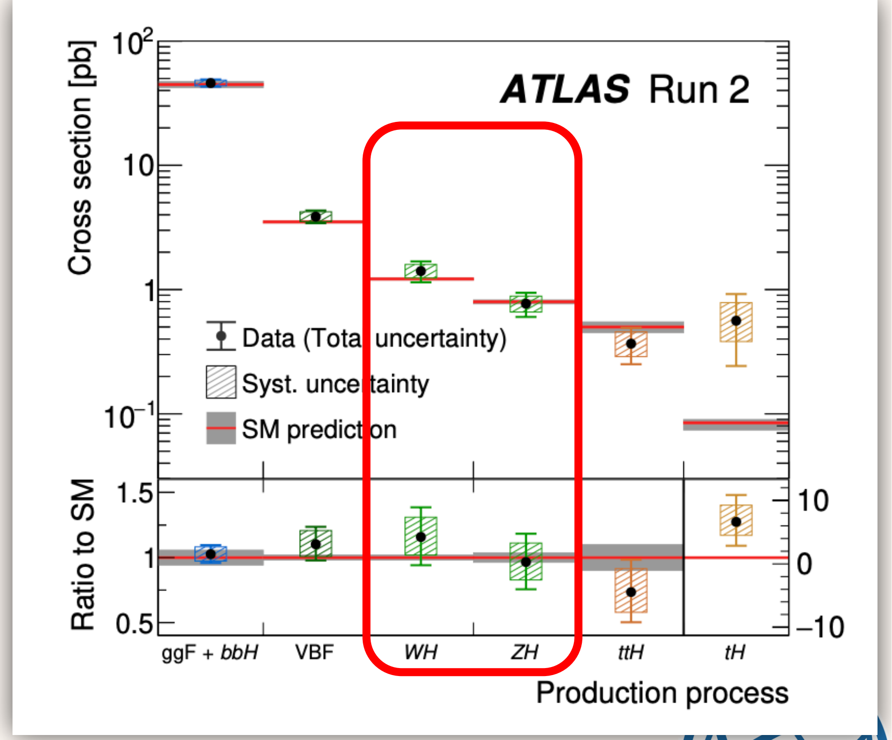

- Thanks to LHC's huge statistic, able to challenge other channels
  - ･ Other Higgs decays (eg. WW, ττ, cc …)

- Key of VH analysis to measure properties with higher precision
  - ➔ Improving particle identification performance
  - ➔ Better constraint on background

VH analyses overview with full Run2 in ATLAS

- Identification framework upgraded: b-jet, c-jet, τ ID, etc…
- **1st** VH measurements performed with full Run2 dataset
  - Integrated luminosity: 140 fb^{-1}, Centre of mass: 13 TeV
- Some **2nd** updated analyses also performed exploiting improved analysis techniques for better precision
- All major Higgs decays in VH production are analysed
- All results are consistent with SM prediction within their uncertainties

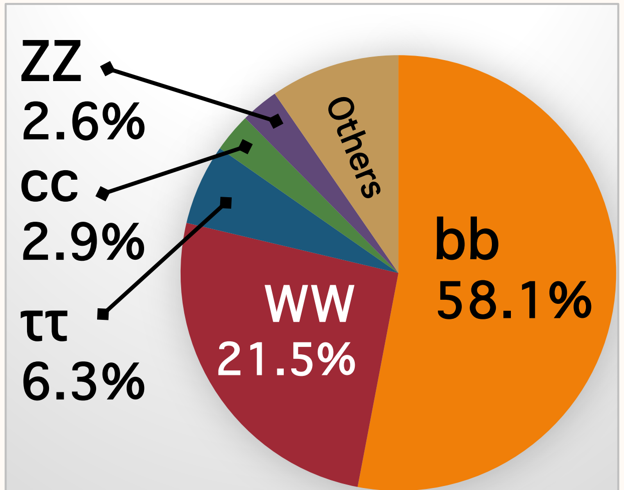

[arXiv:1610.07922v2]

< VH analyses > very new and interesting analyses

2nd	V(lep) ,H(bb/cc)	: ATLAS-CONF-2024-010
1st	V(had) ,H(bb)	: Phys. Rev. Lett. 132 (2024) 131802
2nd	V(lep/had),H(WW)	: ATLAS-CONF-2022-067
1st	V(lep) ,H(ττ)	: Phys. Lett. B 855 (2024) 138817
2nd	V(had) ,H(ττ)	: arXiv:2407.16320
1st	V(lep/had),H(ZZ)	: Eur. Phys. J. C 80 (2020) 957
1st	V(lep/had),H(γγ)	: JHEP 07 (2023) 088
1st	V(lep) ,H(μμ)	: Phys. Lett. B 812 (2021) 135980

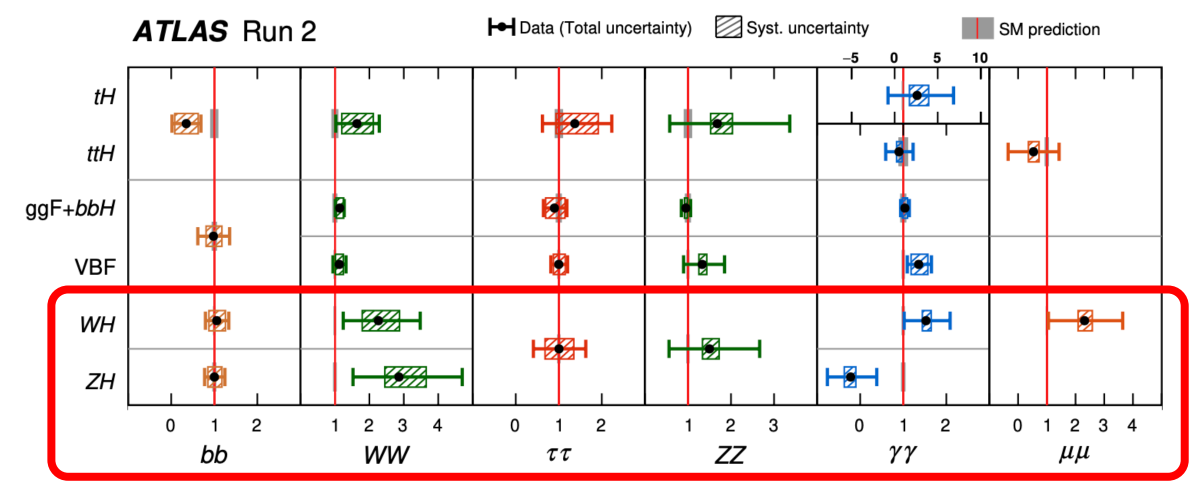

[Nature volume 607, pages 52–59 (2022)]

* **1st** :The first publication for the mode with full Run2, **2nd** :The second publication for the mode with full Run2

VH,H→bb/cc

Very latest V(lep)H->hadron analysis in ATLAS

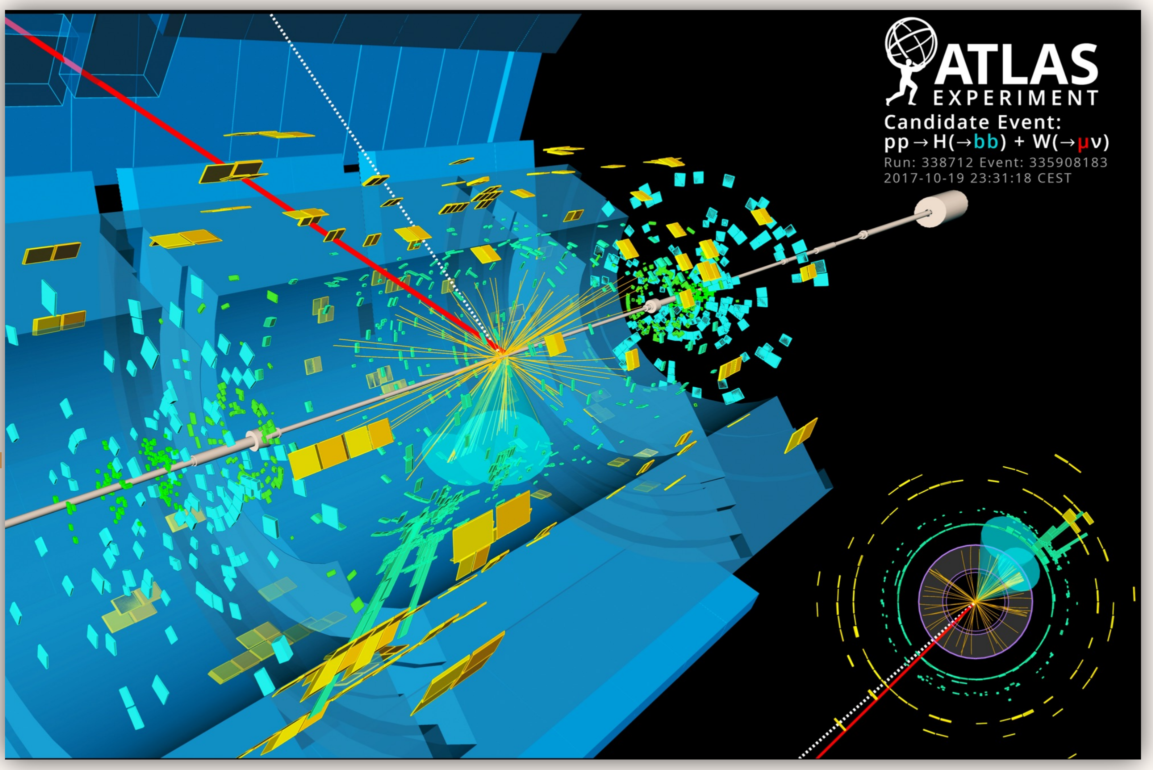

ATLAS Experiment © 2018 CERN

What's new in VH, H→bb/cc analysis?

- Analysis strategy and techniques
  - Combined fit with VH,H→bb and VH,H→cc
    → Better constraint on background events with CRs in VH,H→cc
  - New flavour tagging algorithm
    → Better tagging performance for hadronic final states
  - Final discriminant MVA: Re-optimize in resolved VH,H→bb
    and first apply in VH,H→cc, boosted VH,H→bb
- Results
  - Updated precise measurement of signal strength (μ_{VH}^{bb}, μ_{VH}^{cc}) from previous result *1*2
  - Differential cross-section measurement for VH production
    - Updated result from previous result *1
    - New result with new additional split bins

$$\mu_{VH}^{bb} = \sigma_{VH}^{measured} \times B_{H\to bb}^{measured} \Big/ \sigma_{VH}^{SM} \times B_{H\to bb}^{SM}$$

*1 ATLAS-CONF-2021-051
*2 Eur. Phys. J. C 82 (2022) 71

Analysis strategy

Fit all regions (59 SRs, 97 CRs) simultaneously

Flavour tagging

c-tag

VH, H→cc

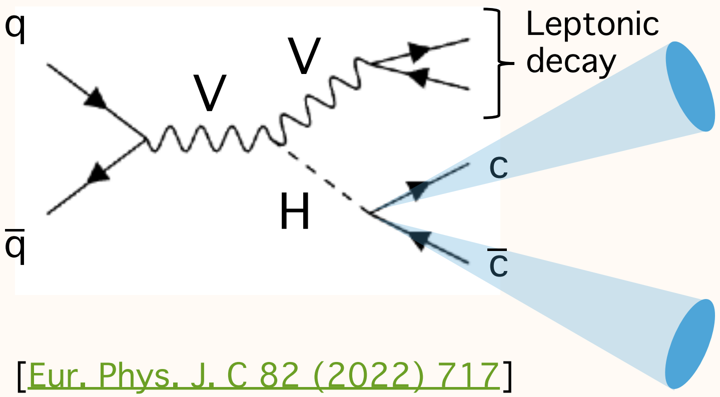

[Eur. Phys. J. C 82 (2022) 717]

Leptonic decay :

Z → νν (0-lepton)

W → lν (1-lepton)

Z → ll (2-lepton)

* l = e, μ (τ in 1-lepton)

b-tag

VH, H→bb resolved

[ATLAS-CONF-2021-051]

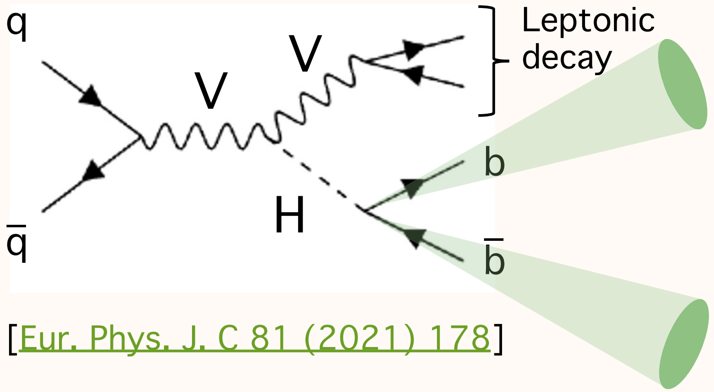

[Eur. Phys. J. C 81 (2021) 178]

VH, H→bb boosted

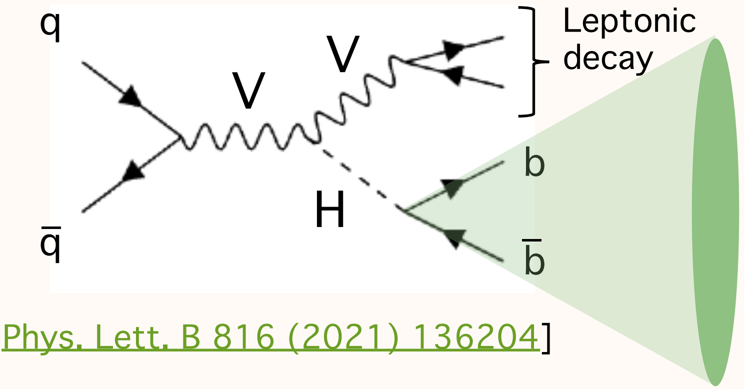

[Phys. Lett. B 816 (2021) 136204]

75 GeV

400 GeV

p_T^V

Flavour tagging

- Updated the flavour tagging algorithm (MV2c → DL1r)
  - ➢ Deep neural network to tag b-, c-, light-jets using b-, c-jet kinematic features as training inputs
- b-tag working point (WP) and c-tag WP are obtained orthogonally

Heavy-flavour-jet feature

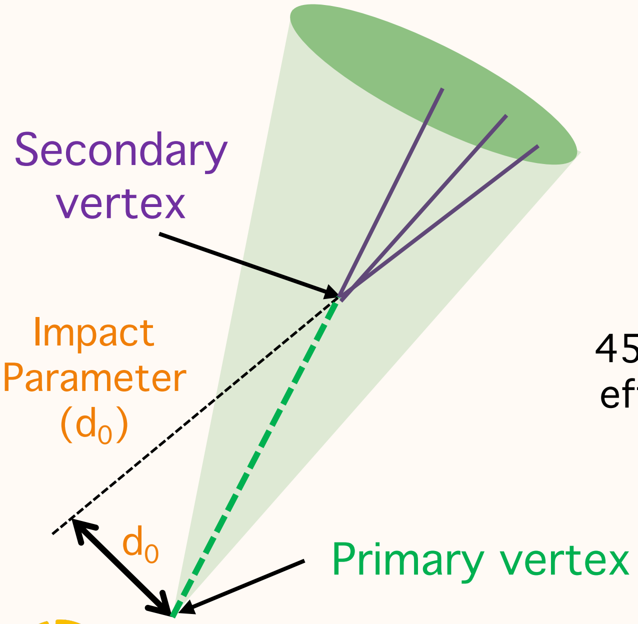

b-tag, c-tag WPs

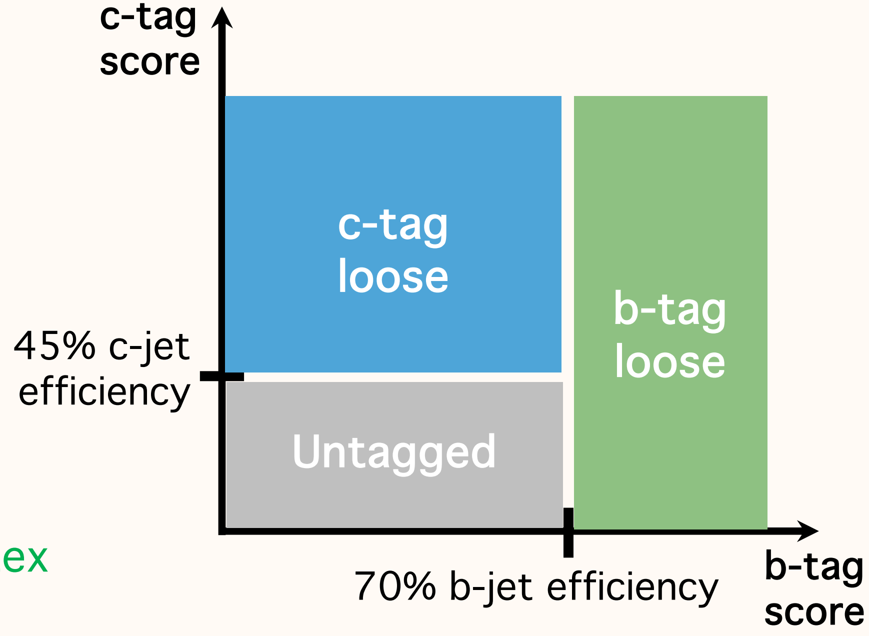

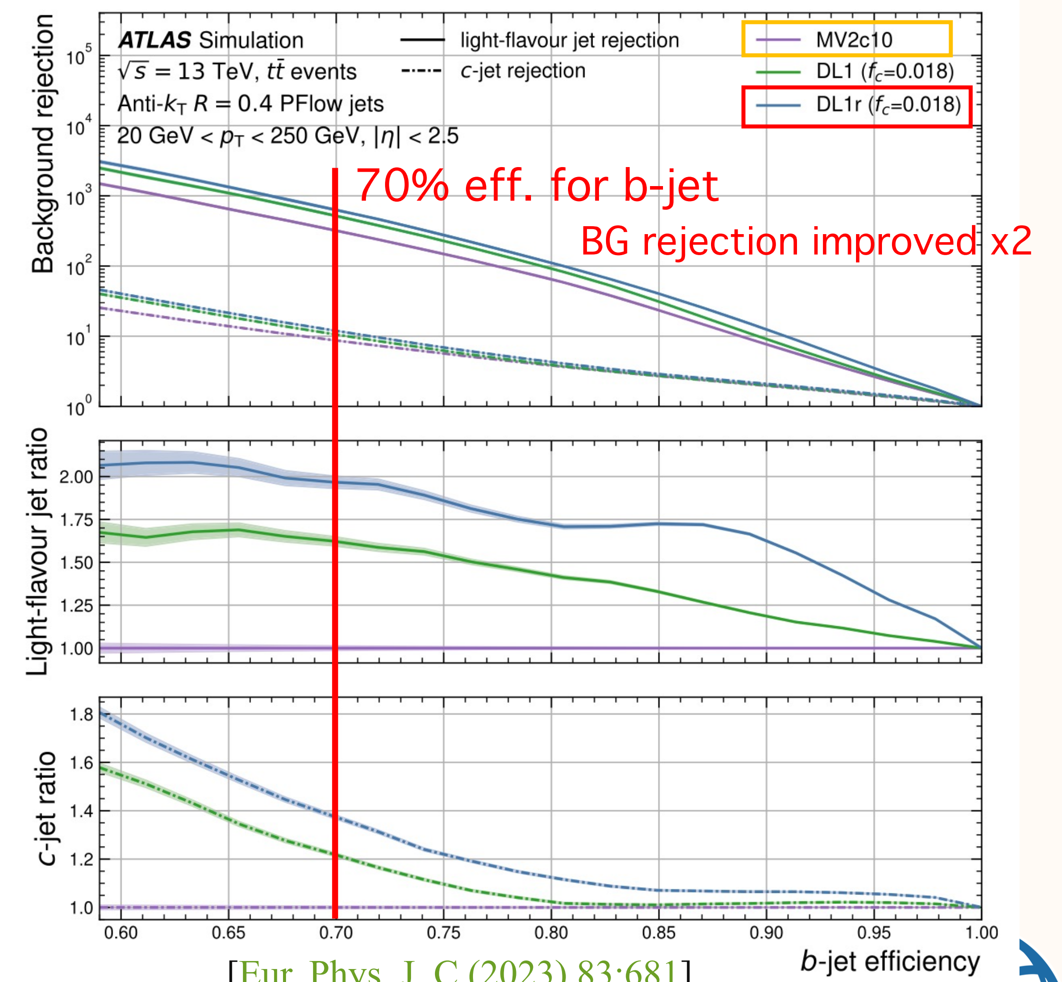

70% eff. for b-jet

BG rejection improved x2

[Eur. Phys. J. C (2023) 83:681]

Inclusive result of VH,H→bb

All plots [ATLAS-CONF-2024-010]

- Fitted signal and background get good closure with data
- Uncertainty of signal strength estimation (VH,H→bb) ~15 %
  - ➢ Improved ~14 % from previous analysis [ATLAS-CONF-2021-051]
- WH,H→bb observed first time

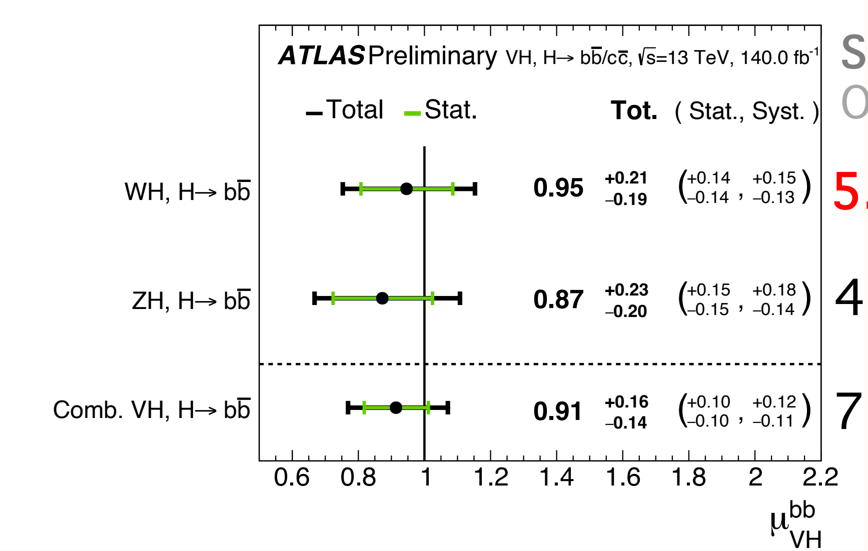

Significance
Obs.(Exp.)

5.3(5.5)σ

4.9(5.7)σ

7.4(8.0)σ

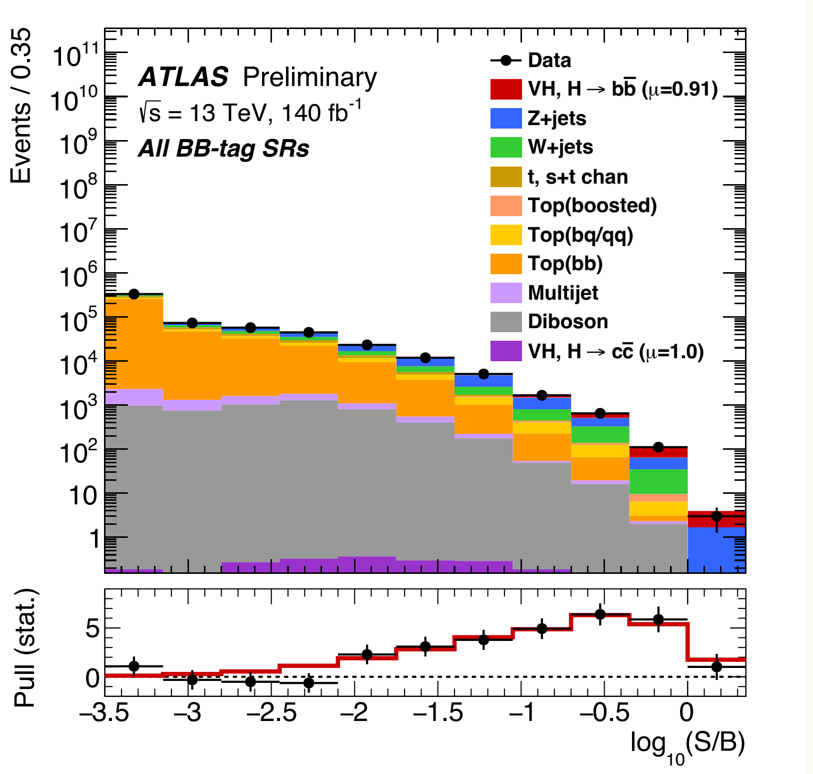

Inclusive result of VH,H→cc

All plots [ATLAS-CONF-2024-010]

- Fitted signal and background get good closure with data
- VH,H→cc observed (expected) limits at 95 % CL: 11.2 (10.4) x SM
  - ➢ Improved x 3 from previous analysis [Eur. Phys. J. C 82 (2022) 717]
- As cross-check of this analysis, VZ,Z→cc first observed; 5.2σ

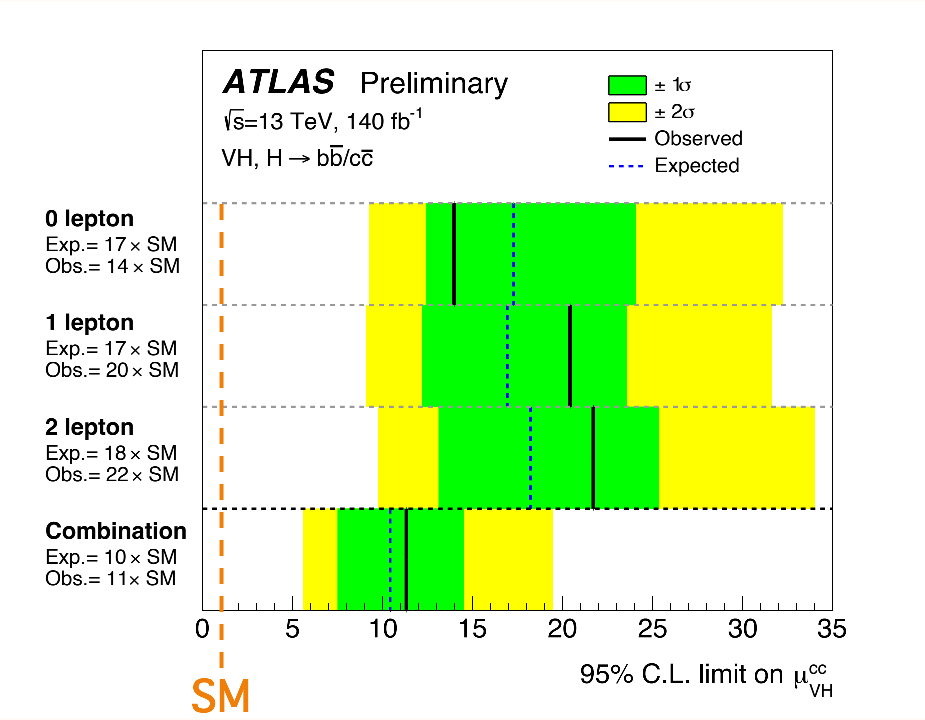

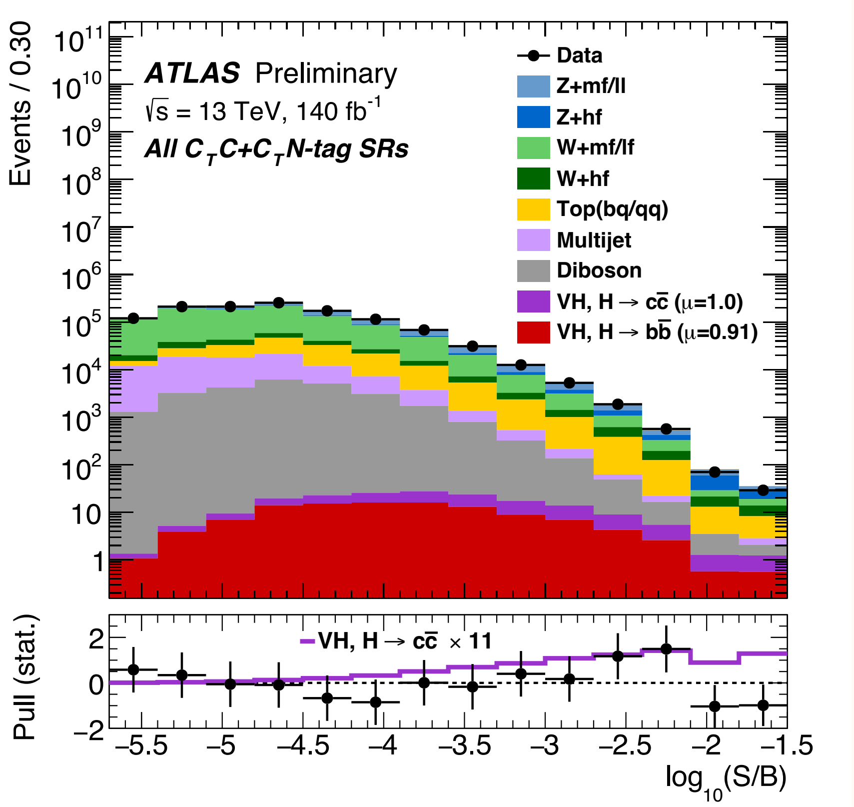

Fiducial differential cross-section measurement

- Since enough statistic available in V(lep)H,H->bb,
  fiducial differential cross-section measurement also performed

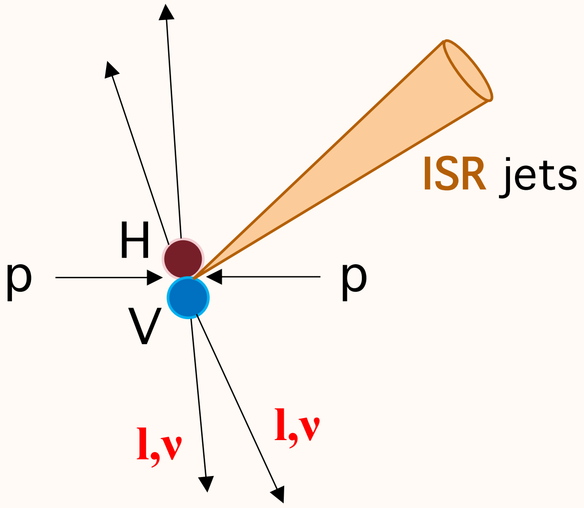

- Simplified Template Cross-Section (STXS) framework
  - Divide phase space into simplified “bins”
  - STXS bins defined by whole LHC group
    - Minimize theoretical dependency
    - Maximize BSM sensitivity
    - Combine ATLAS and CMS results to verify theory models
- p_T^V bin
  - BSM sensitivity in High p_T^V region after SMEFT interpretation
- ISR nJet bin
  - Reduce QCD scale’s huge variation

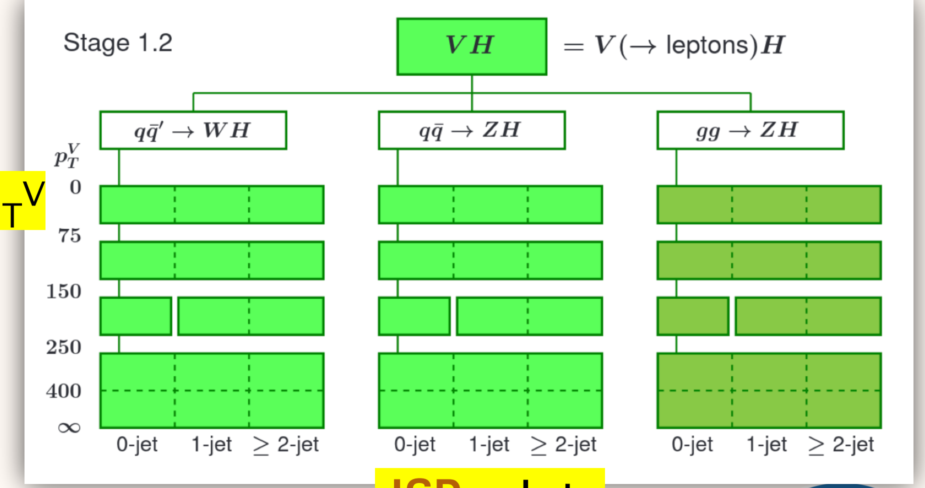

p_T^V

ISR nJets

Updated STXS result (only split in p_T^V)

- Added new bin; WH, $75 < p_T^{W,t} < 150$ GeV
- New split in high p_T region; $p_T > 600$ GeV

- Good agreement with SM prediction
- Uncertainty of observed cross-section in major bins: ~30 - ~80 %

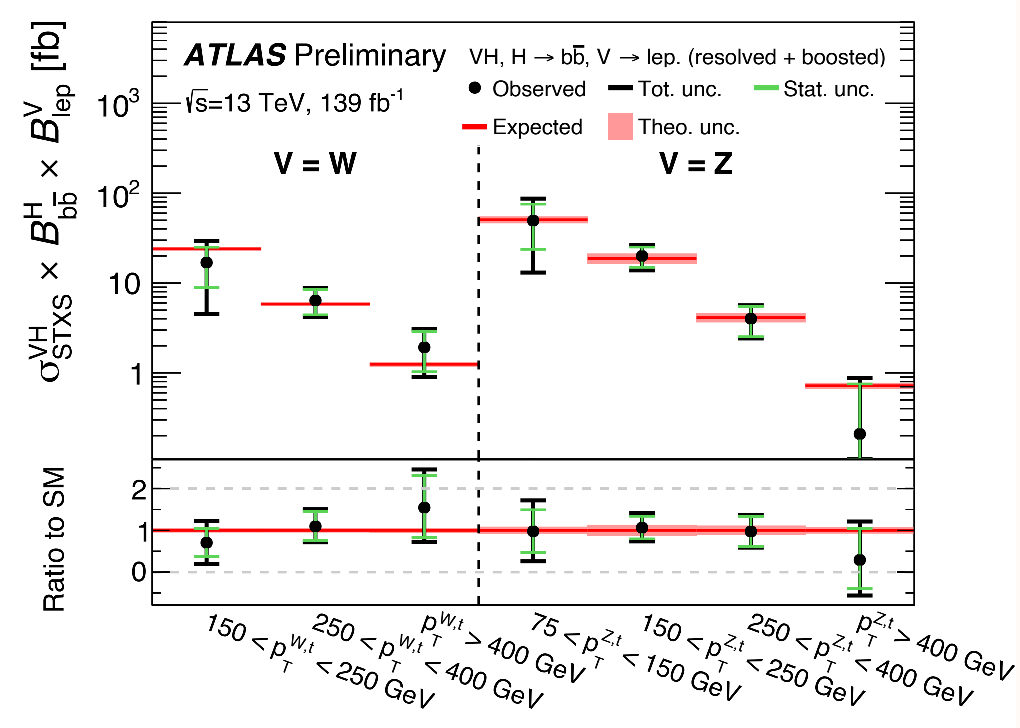

[ATLAS-CONF-2021-051]

Uncertainty: max. ~10 % improved in the same bin

p_T^V spectrum cross-section plot

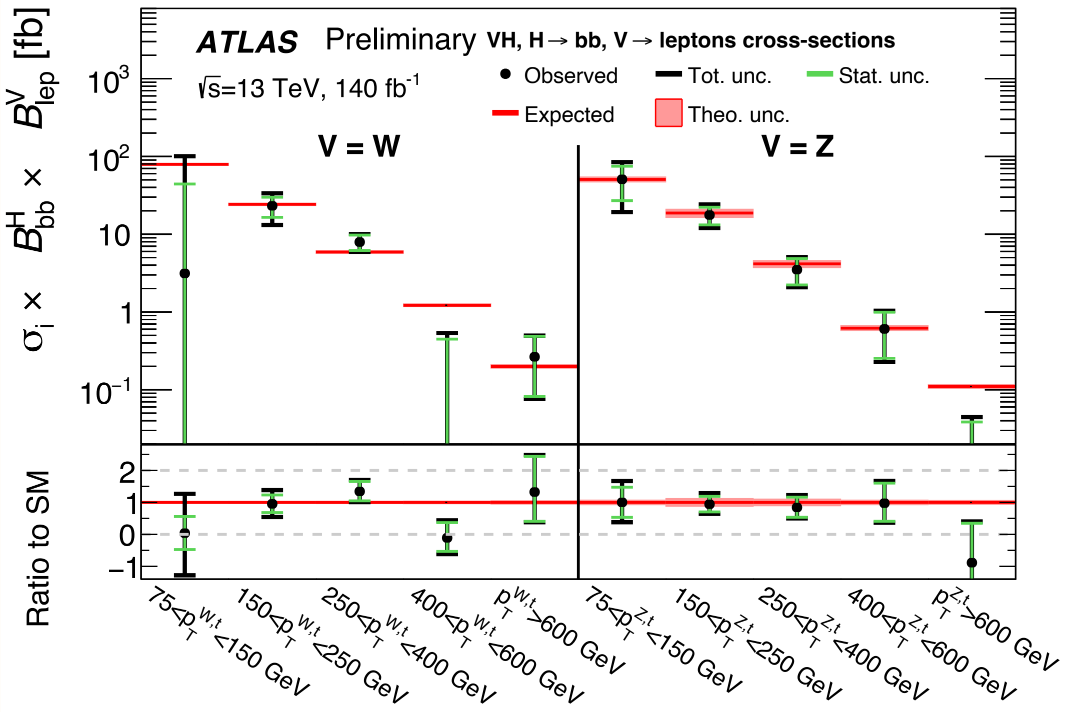

[ATLAS-CONF-2024-010]

New STXS result (split in p_T^V x nJet)

- New split with number of additional jets (nJets)

- The statistics of ZH is enough to split with nJets
- Good agreement with SM prediction
- Uncertainty of ZH, nJ = 0 bins: ~50 %
- Uncertainty of ZH, nJ ≧ 1 bins: ~60 - ~400 %

- In the future, STXS bin in WH will split with nJets with enough statistic

p_T^V x nJ(ZH) spectrum cross-section plot

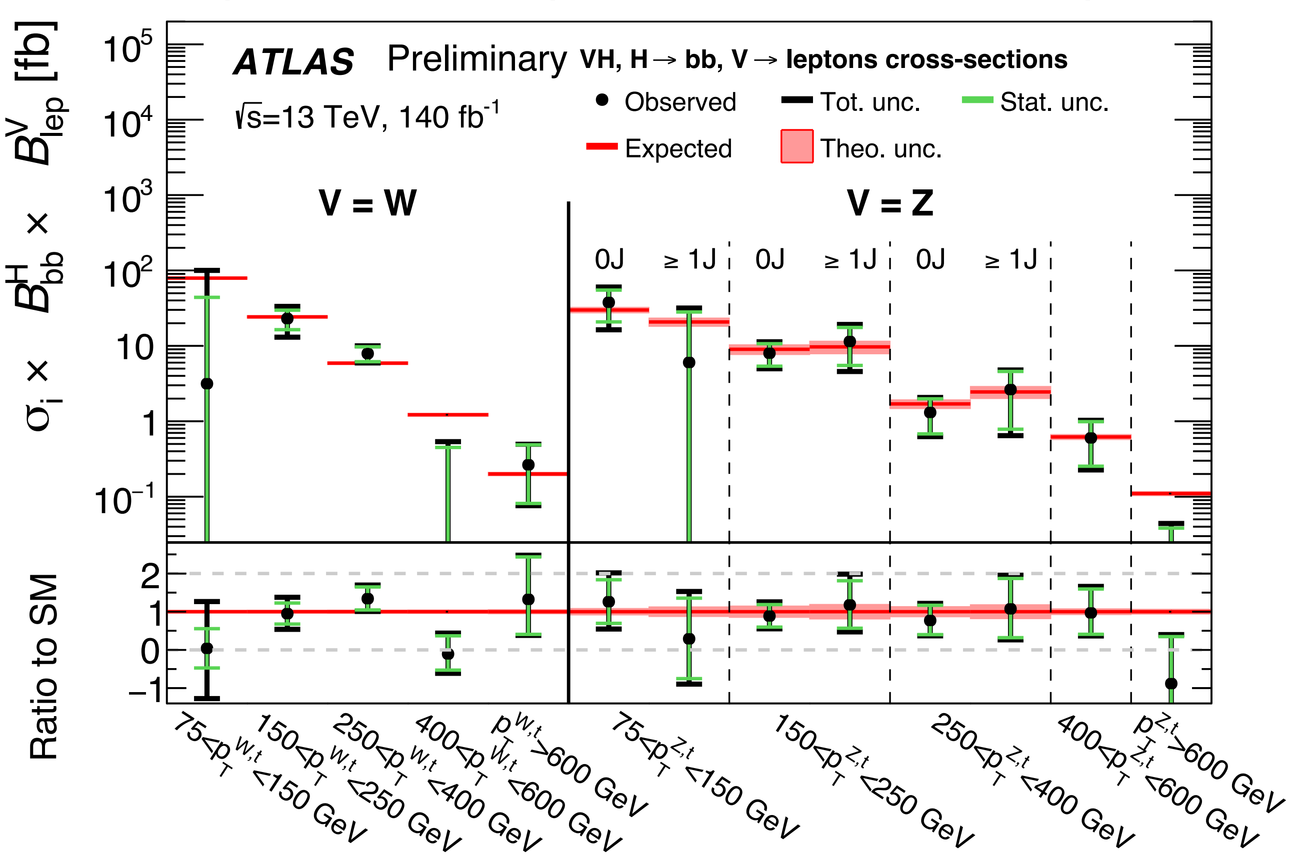

[ATLAS-CONF-2024-010]

Latest results of the other VH measurements

Thanks to

- Improved particle identification framework in the ATLAS
- (For rare decays' analyses) LHC's huge statistic

Analyses of other channels

- V(had)H, H→ bb analysis [Phys. Rev. Lett. 132 (2024) 131802]

$$\mu_{VH}^{bb} = 1.39\,^{+1.02}_{-0.88} \quad \binom{+0.63}{-0.63}\,stat.\binom{+0.80}{-0.61}\,syst.$$

  - ➢ Measured signal strength is consistent with SM prediction
  - ➢ Systematic uncertainty is dominant
    - Major uncertainties: b-tag scale factor, data-driven multi-jet estimation

    → More chance for precise measurement in boosted all-hadronic phase space

- V(lep/had)H, H→WW analysis [ATLAS-CONF-2022-067]

$$\mu_{VH}^{WW} = 0.92\,^{+0.25}_{-0.23} \quad \binom{+0.21}{-0.20}\,stat.\binom{+0.13}{-0.11}\,syst.$$

  - ➢ Combined V(leptonic decay)*1 and V(hadronic decay) analyses
  - ➢ Measured signal strength is consistent with SM prediction
  - ➢ Statistical uncertainty is dominant

---

*1 Phys. Lett. B **798** (2019) 134949

Analyses relating to H→ττ

- Hadronic tau (τ_{had}) identification upgraded from BDT-based to RNN-based
  - New framework, widely used in τ_{had}-related analyses in the ATLAS

- V(lep)H, H→ ττ analysis [Phys. Lett. B 855 (2024) 138817]

$$\mu_{VH}^{\tau\tau} = 1.28\,^{+0.39}_{-0.36} \begin{pmatrix}+0.30\\-0.29\end{pmatrix} stat. \begin{pmatrix}+0.25\\-0.21\end{pmatrix} syst.$$

  - Measured signal strength is consistent with SM prediction
  - Statistical uncertainty is dominant

- V(had)H, H→ττ analysis [arXiv:2407.16320]

$$\mu_{VH}^{\tau\tau} = 0.91\,^{+0.63}_{-0.60} \begin{pmatrix}+0.53\\-0.51\end{pmatrix} stat. \begin{pmatrix}+0.35\\-0.33\end{pmatrix} syst.$$

  - Measured signal strength is consistent with SM prediction
  - Statistical uncertainty is dominant

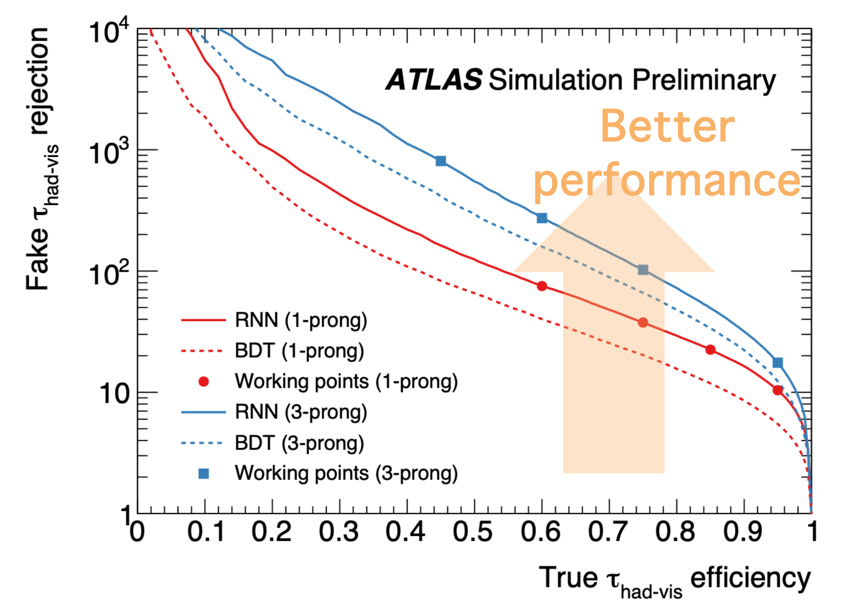

[ATL-PHYS-PUB-2019-033]

Recap of full Run2 VH measurement results

VH Analyses		Inclusive Signal strength (μ)	Observed Significance	References
2nd	V(lep) ,H(bb/cc)	$\mu_{VH}^{bb} = 0.91\,^{+0.16}_{-0.14}$ $\mu_{VH}^{cc} = 1.0\,^{+5.4}_{-5.2}$	7.4 σ (95% CL upper limit 11.3 xSM)	**ATLAS-CONF-2024-010**
1st	V(had) ,H(bb)	$\mu_{VH}^{bb} = 1.39\,^{+1.02}_{-0.88}$	1.7 σ	**Phys. Rev. Lett. 132 (2024) 131802**
2nd	V(lep/had),H(WW)	$\mu_{VH}^{WW} = 0.92\,^{+0.25}_{-0.23}$	4.6 σ	**ATLAS-CONF-2022-067**
1st	V(lep) ,H(ττ)	$\mu_{VH}^{\tau\tau} = 1.28\,^{+0.39}_{-0.36}$	4.2 σ	**Phys. Lett. B 855 (2024) 138817**
2nd	V(had) ,H(ττ)	$\mu_{VH}^{\tau\tau} = 0.91\,^{+0.63}_{-0.60}$	(Not published)	**arXiv:2407.16320**
1st	V(lep/had),H(ZZ)	$\mu_{VH}^{ZZ} = 1.43\,^{+1.16}_{-0.94}$	(Not published)	**Eur. Phys. J. C 80 (2020) 957**
1st	V(lep/had),H(γγ)	$\mu_{WH}^{\gamma\gamma} = 1.5\,^{+0.6}_{-0.5}$ $\mu_{ZH}^{\gamma\gamma} = -0.2\,^{+0.6}_{-0.5}$	(Not published)	**JHEP 07 (2023) 088**
1st	V(lep) ,H(μμ)	$\mu_{VH}^{\mu\mu} = 5.0\,^{+3.5}_{-3.5}$	(1.2 σ) (combined H production)	**Phys. Lett. B 812 (2021) 135980**

* **1st** :The first publication for the mode with full Run2, **2nd** :The second publication for the mode with full Run2

Conclusion

- Latest and wonderful results for VH production measurement are available with full Run2 dataset with the ATLAS experiment
    - ➢ Thanks to LHC's huge statistic and updated particle identification used in the ATLAS
- All results are consistent with SM prediction

H→bb : Systematic uncertainty dominant; New analysis technique demanded

Other decays : Statistic limited; Looking forward to seeing results with Run3 dataset !!

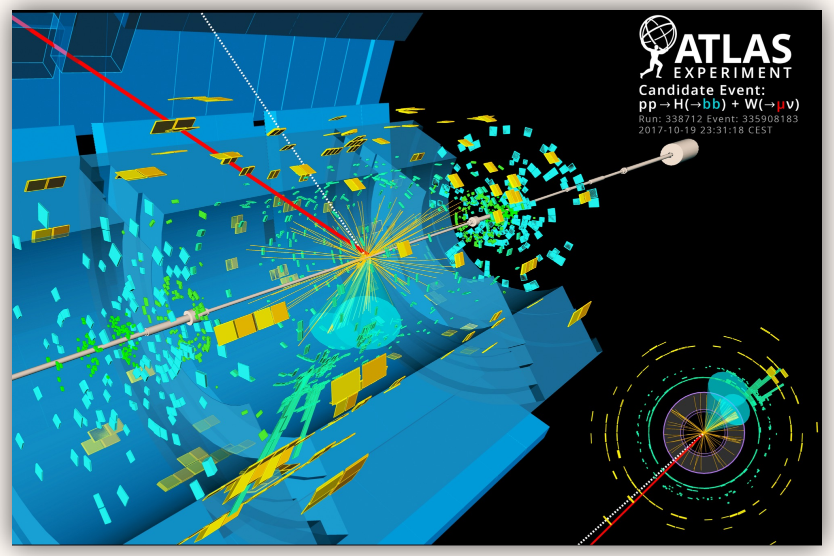

W(lep)H,H→bb

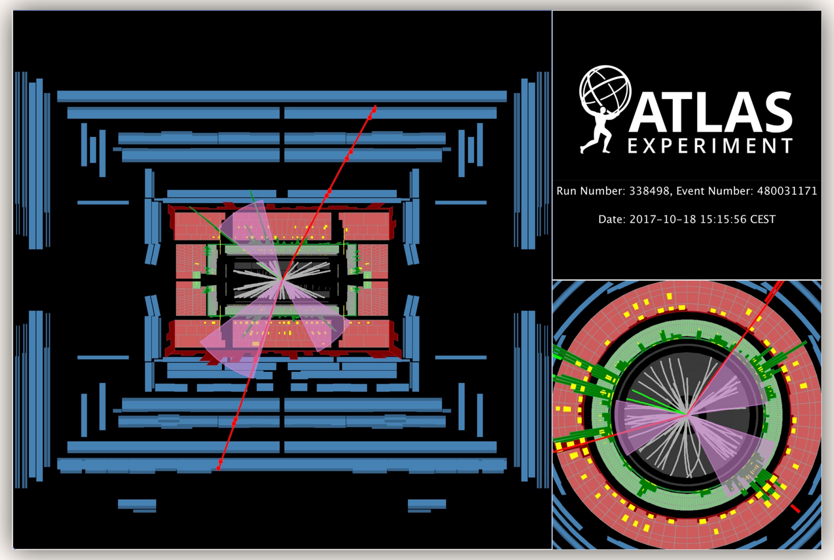

V(had)H,H→2μ2e

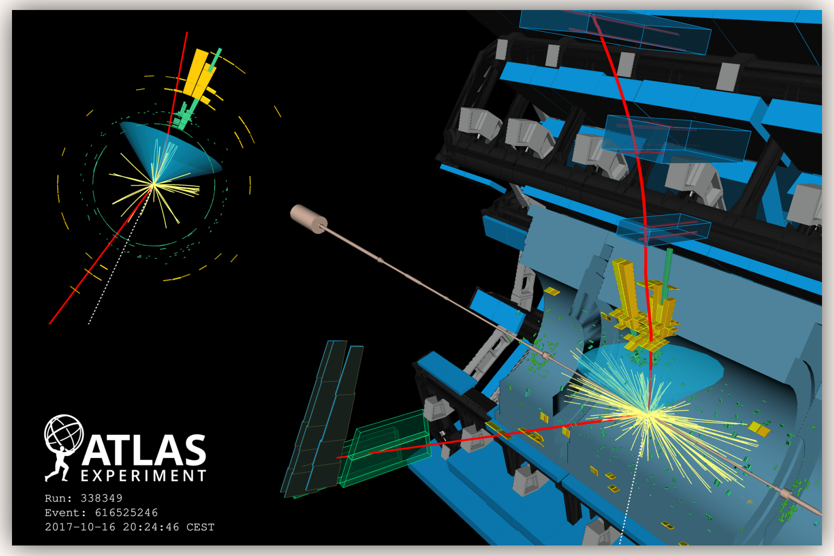

W(lep)H,H→bb boosted

by Steve Jurvetson - The Spanish Fortress in Hvar, Croatia

Backup

V(lep/had)H, H→WW analysis - strategy

- 4 channels to target different signal signature (Total 8 regions)
- MVA is used in all regions [ATLAS-CONF-2022-067]

*1 previous: Phys. Lett. B **798** (2019) 134949

[VH opposite-sign 2L]

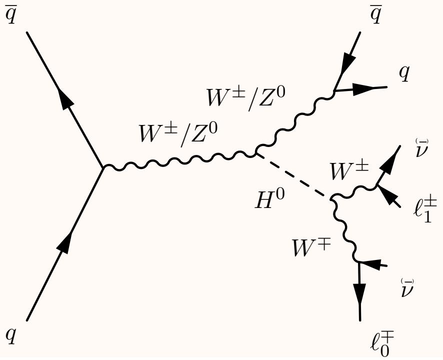

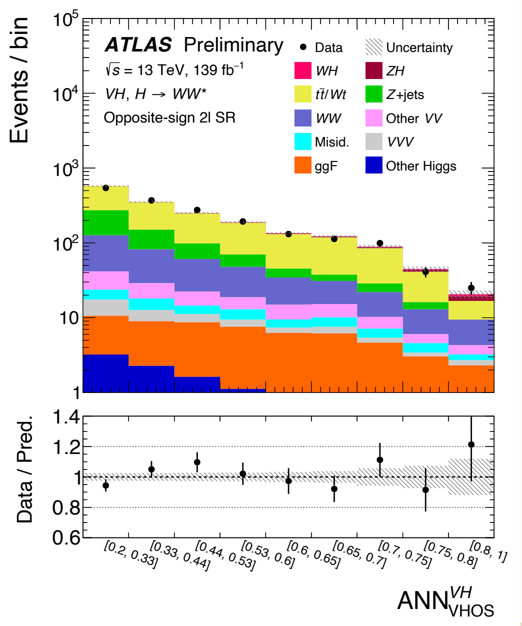

[WH same-sign 2L]
{SS2μ, SS2e, SSDF}

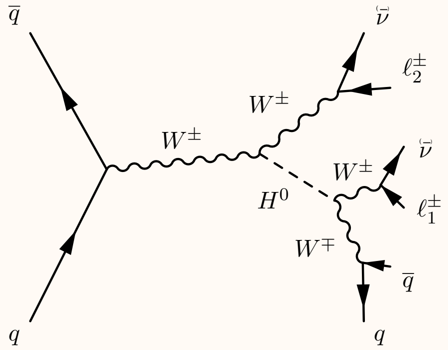

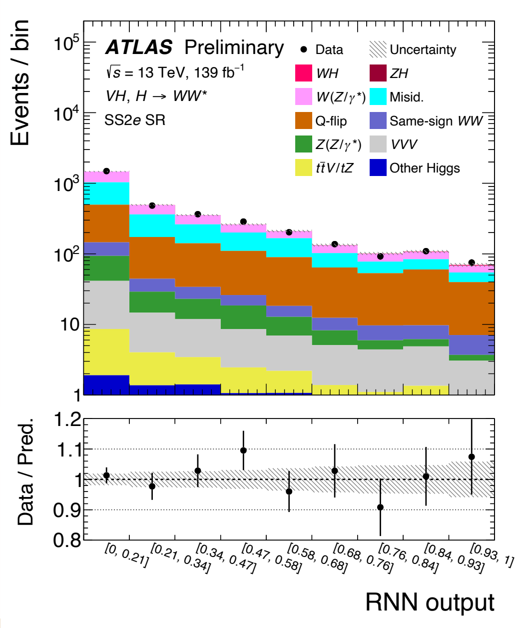

[WH 3L] *1
{Z-dominant, Z-depleted}

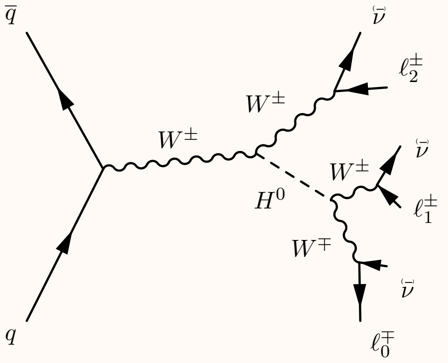

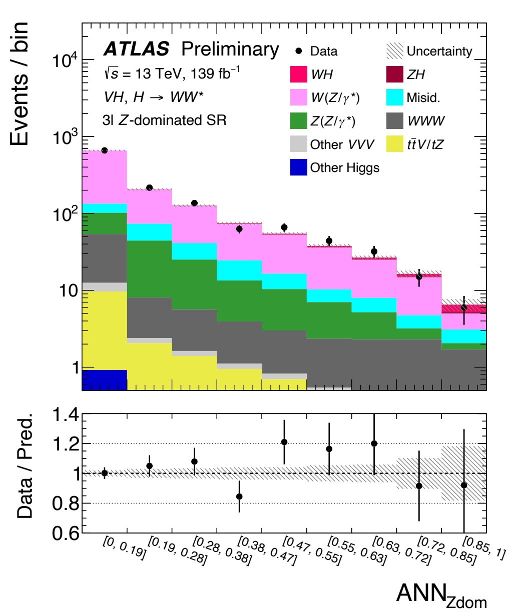

[ZH 4L] *1
{1-SFOS, 2-SFOS}

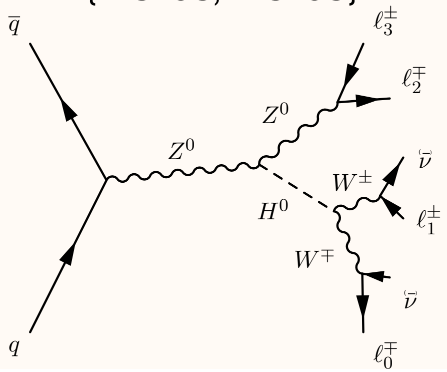

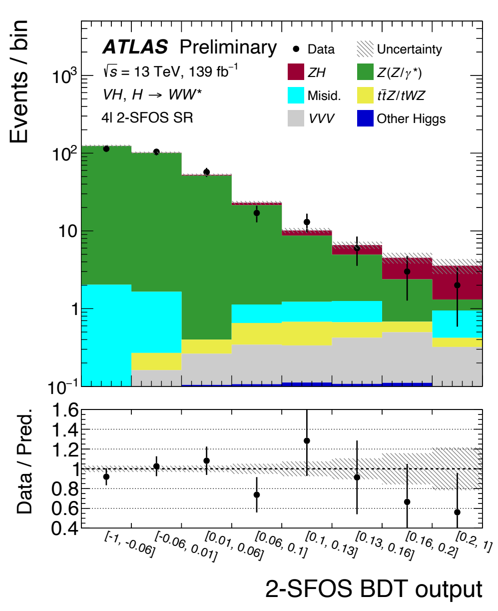

V(lep/had)H, H→WW analysis - results

[ATLAS-CONF-2022-067]

- Statistical uncertainty is dominant in all POIs
- Inclusive (VH) signal strength is consistent with SM prediction within its uncertainty

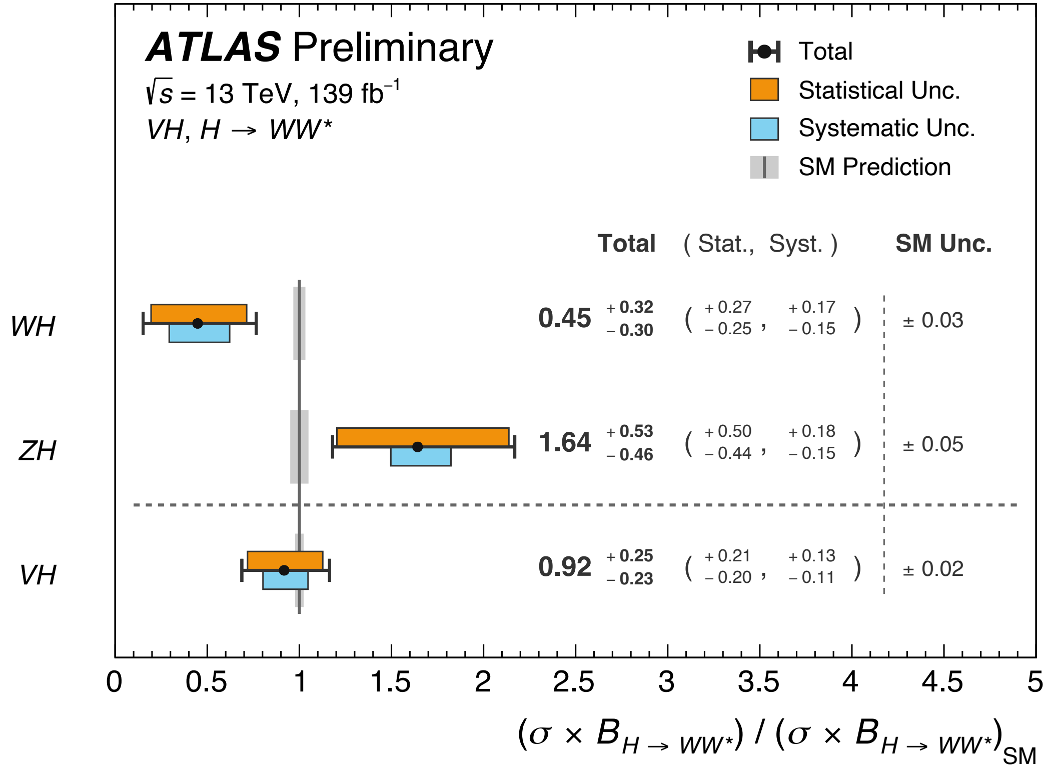

Significance

Obs.(Exp.)

1.5(3.3)σ

4.6(3.1)σ

4.6(4.7)σ

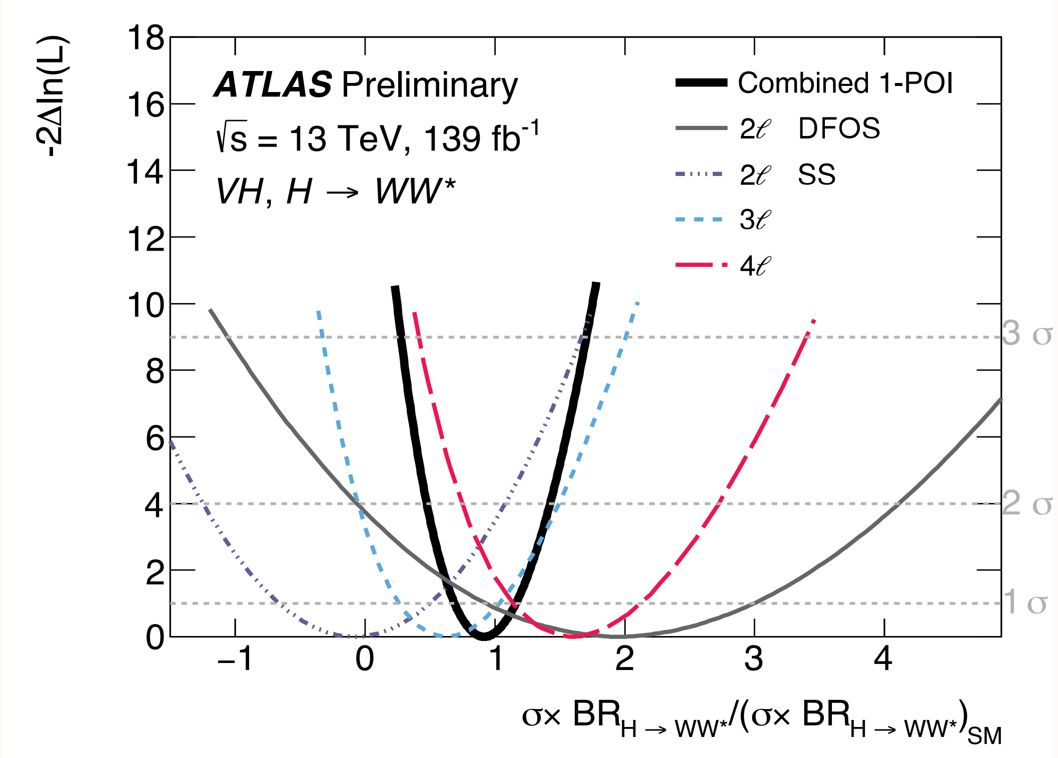

V(lep)H, H→ττ analysis

[ATL-PHYS-PUB-2019-033]

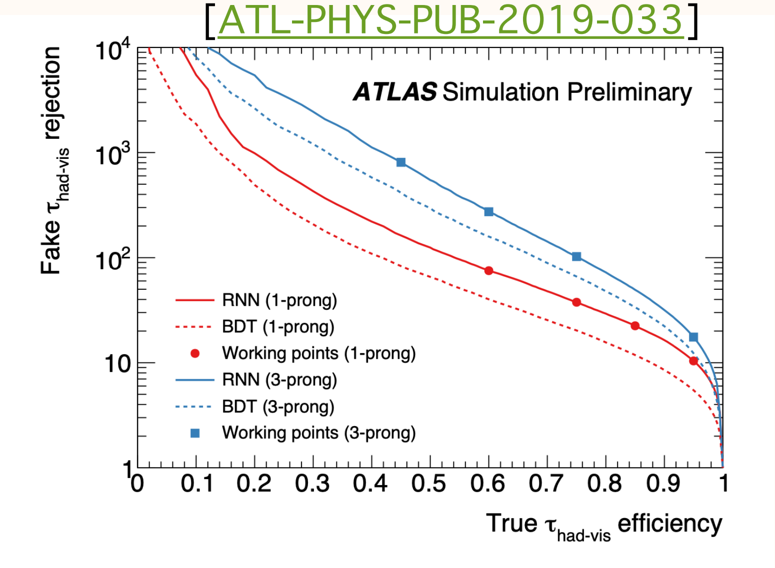

- τ_{had} identification upgraded from BDT-based to RNN-based
- Fit simultaneously in 4 regions (ZH, WH) × ($\tau_{had}\tau_{had}$, $\tau_{lep}\tau_{had}$)
- Neural Network used for final discriminant variable

- Fitted signal and background get good agreement with data
- Statistical uncertainty is still dominant

[Phys. Lett. B 855 (2024) 138817]

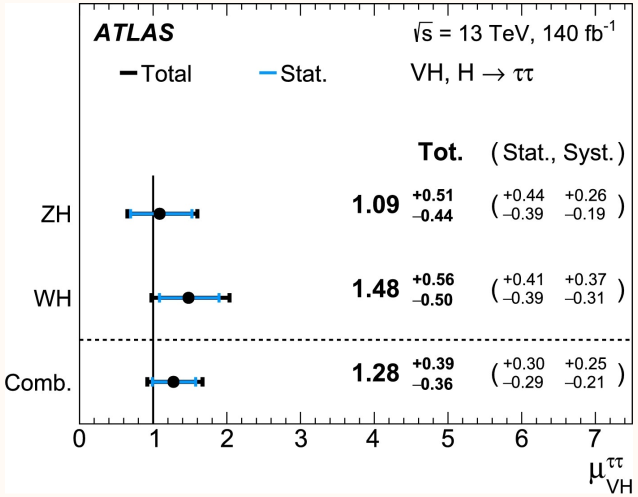

Significance

Obs.(Exp.)

4.2(3.6)σ

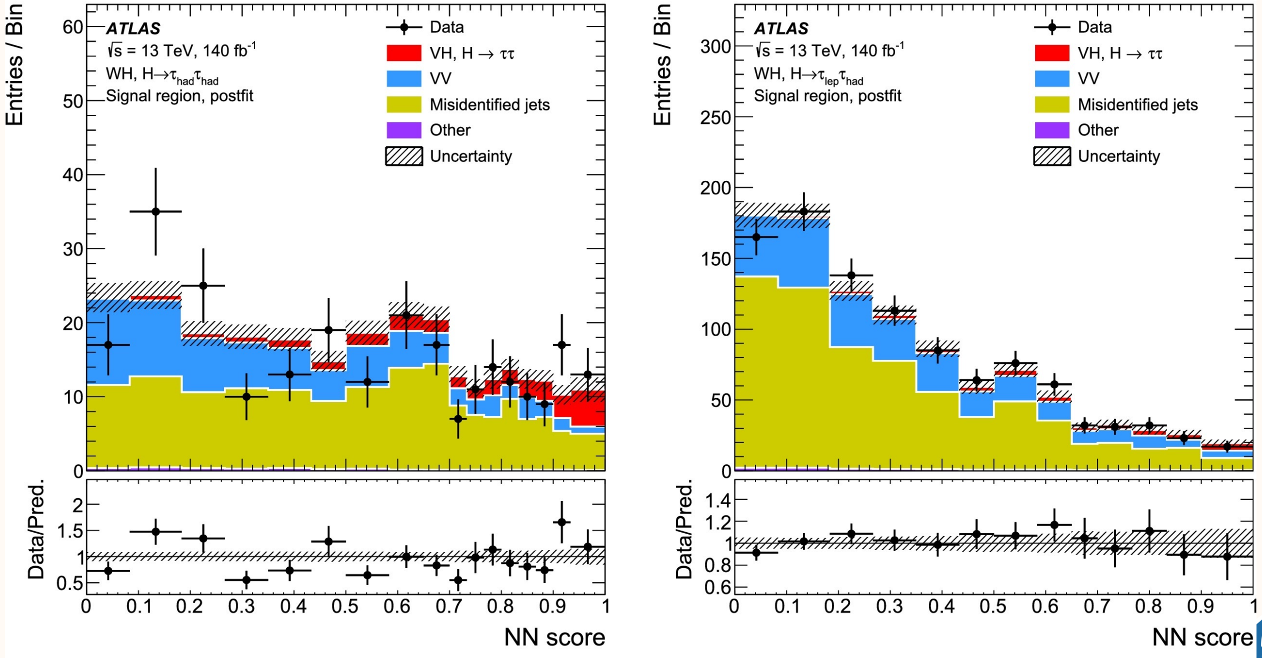

V(had)H, H→ττ analysis

This analysis focused on the STXS measurement in ggF, VBF production, which have enough statistic

VH results
- No big update from previous analysis [JHEP 08 (2022) 175]
- Statistical uncertainty is dominant

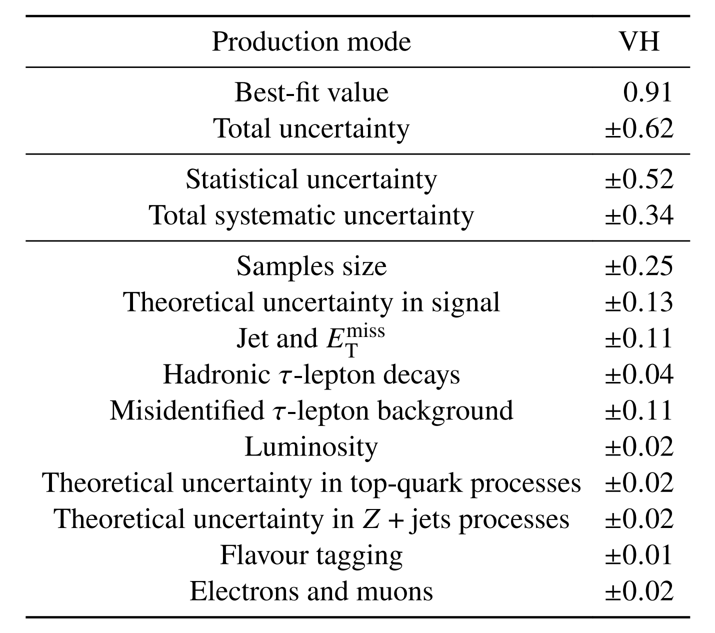

Production mode	VH
Best-fit value	0.91
Total uncertainty	±0.62
Statistical uncertainty	±0.52
Total systematic uncertainty	±0.34
Samples size	±0.25
Theoretical uncertainty in signal	±0.13
Jet and $E_{\mathrm{T}}^{\mathrm{miss}}$	±0.11
Hadronic τ-lepton decays	±0.04
Misidentified τ-lepton background	±0.11
Luminosity	±0.02
Theoretical uncertainty in top-quark processes	±0.02
Theoretical uncertainty in Z + jets processes	±0.02
Flavour tagging	±0.01
Electrons and muons	±0.02

[arXiv:2407.16320]

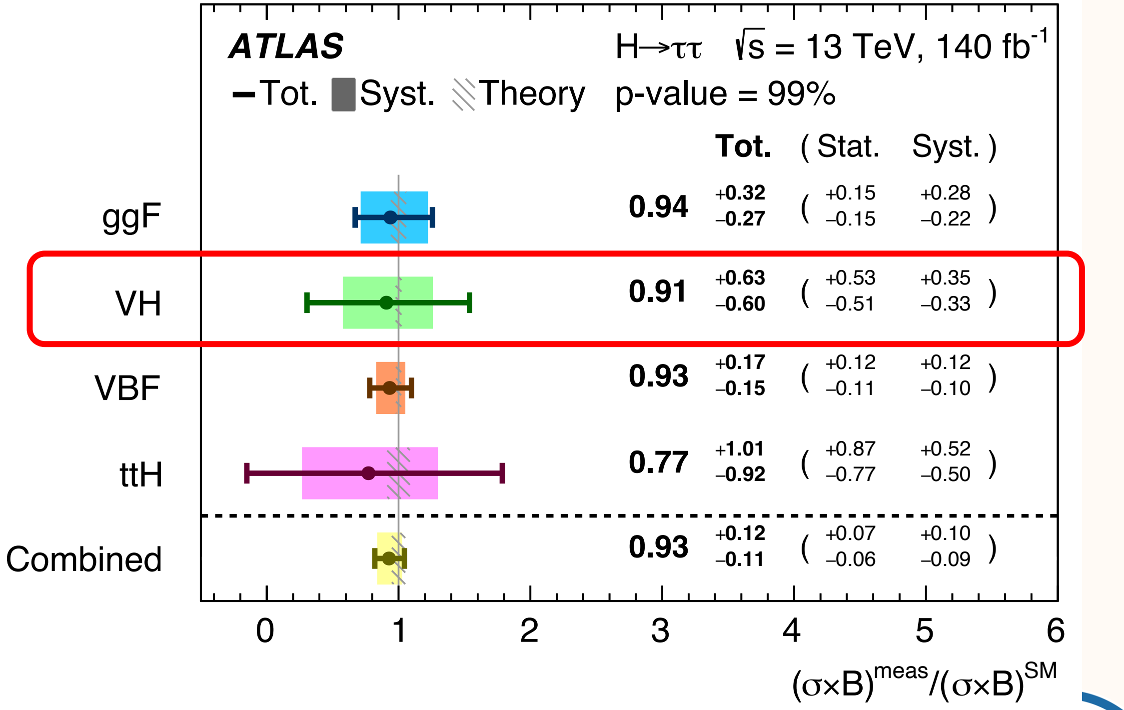

VH, H→bb/cc

* V(lep)H(bb/cc) shown in the ICHEP 2024 by Francesco

* V(had)H(bb) shown in the Higgs Hunting 2023 by Andrea

Profit of STXS measurement

$$\mathcal{L}_{\text{SMEFT}} = \mathcal{L}_{\text{SM}} + \sum_i \frac{c_i^{(D)}}{\Lambda^{D-4}} Q_i^{(D)},$$

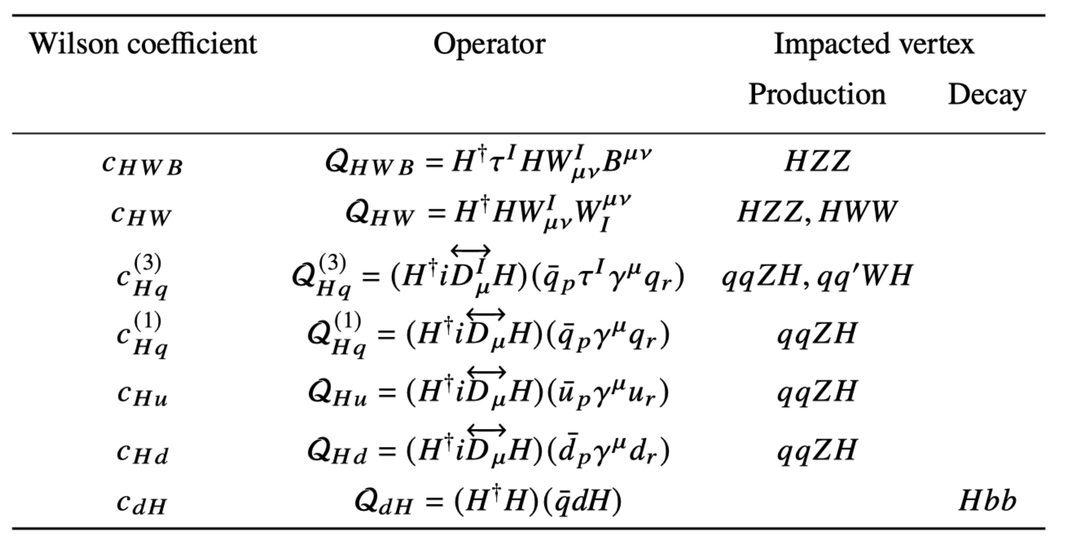

Wilson coefficient	Operator	Impacted vertex	
		Production	Decay
c_{HWB}	$Q_{HWB} = H^\dagger \tau^I H W^I_{\mu\nu} B^{\mu\nu}$	HZZ	
c_{HW}	$Q_{HW} = H^\dagger H W^I_{\mu\nu} W_I^{\mu\nu}$	HZZ, HWW	
$c^{(3)}_{Hq}$	$Q^{(3)}_{Hq} = (H^\dagger i \overleftrightarrow{D}^I_\mu H)(\bar{q}_p \tau^I \gamma^\mu q_r)$	$qqZH, qq'WH$	
$c^{(1)}_{Hq}$	$Q^{(1)}_{Hq} = (H^\dagger i \overleftrightarrow{D}_\mu H)(\bar{q}_p \gamma^\mu q_r)$	$qqZH$	
c_{Hu}	$Q_{Hu} = (H^\dagger i \overleftrightarrow{D}_\mu H)(\bar{u}_p \gamma^\mu u_r)$	$qqZH$	
c_{Hd}	$Q_{Hd} = (H^\dagger i \overleftrightarrow{D}_\mu H)(\bar{d}_p \gamma^\mu d_r)$	$qqZH$	
c_{dH}	$Q_{dH} = (H^\dagger H)(\bar{q} d H)$		Hbb

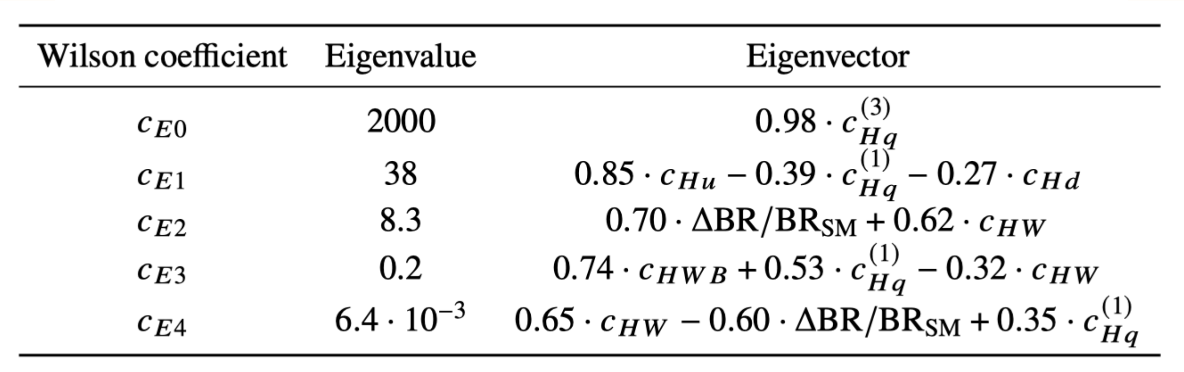

Wilson coefficient	Eigenvalue	Eigenvector
c_{E0}	2000	$0.98 \cdot c^{(3)}_{Hq}$
c_{E1}	38	$0.85 \cdot c_{Hu} - 0.39 \cdot c^{(1)}_{Hq} - 0.27 \cdot c_{Hd}$
c_{E2}	8.3	$0.70 \cdot \Delta\text{BR}/\text{BR}_{\text{SM}} + 0.62 \cdot c_{HW}$
c_{E3}	0.2	$0.74 \cdot c_{HWB} + 0.53 \cdot c^{(1)}_{Hq} - 0.32 \cdot c_{HW}$
c_{E4}	$6.4 \cdot 10^{-3}$	$0.65 \cdot c_{HW} - 0.60 \cdot \Delta\text{BR}/\text{BR}_{\text{SM}} + 0.35 \cdot c^{(1)}_{Hq}$

[Eur. Phys. J. C 81 (2021) 178]

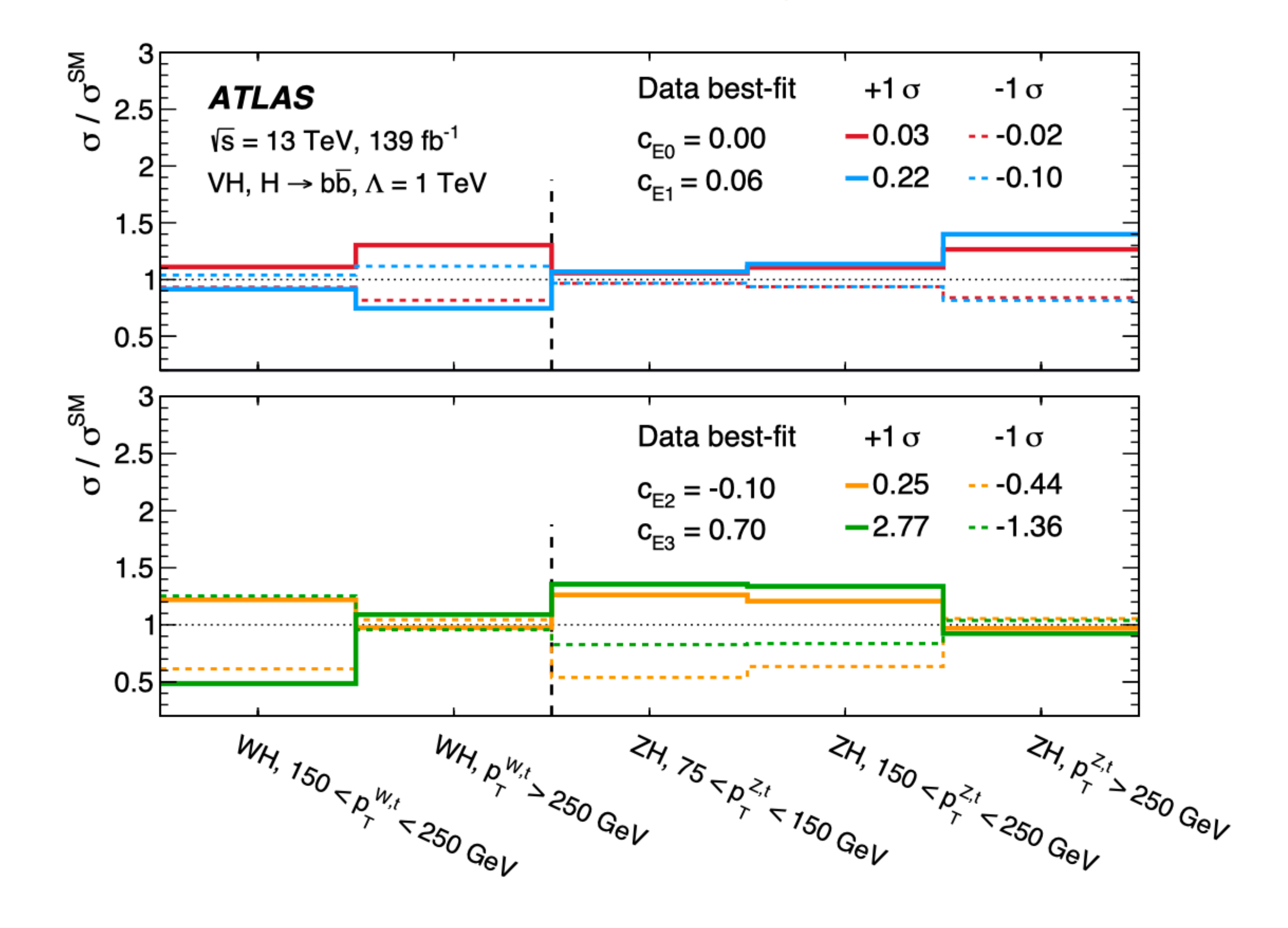

Main background events

ttbar 0,1,2-lepton

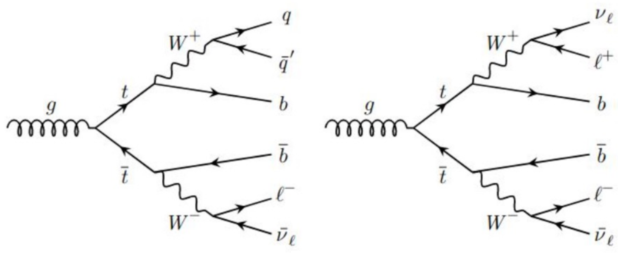

W+jets 0,1-lepton

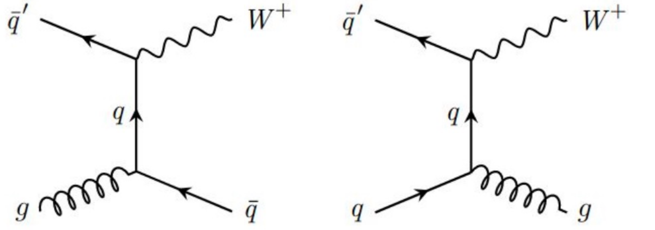

single top 0,1,2-lepton

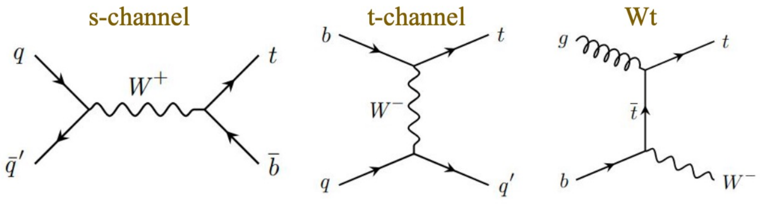

Z+jets 0,2-lepton

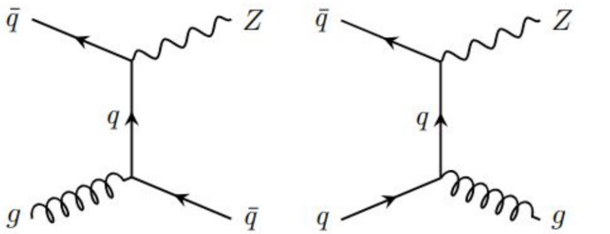

Diboson (VZ) 0,1,2-lepton

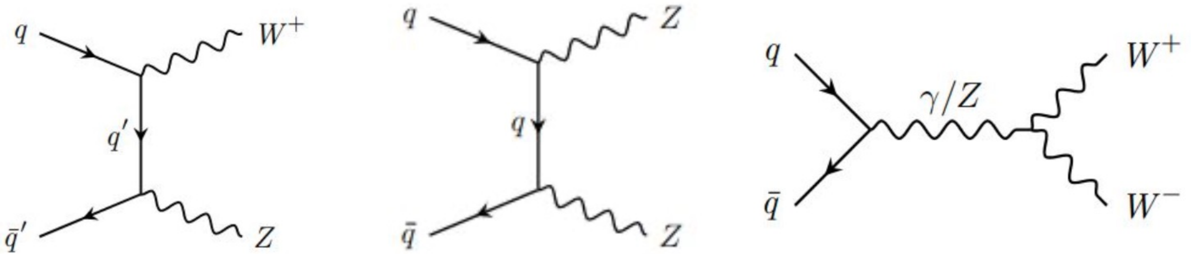

Z->bb, Mbb=~90 GeV

Event categorization

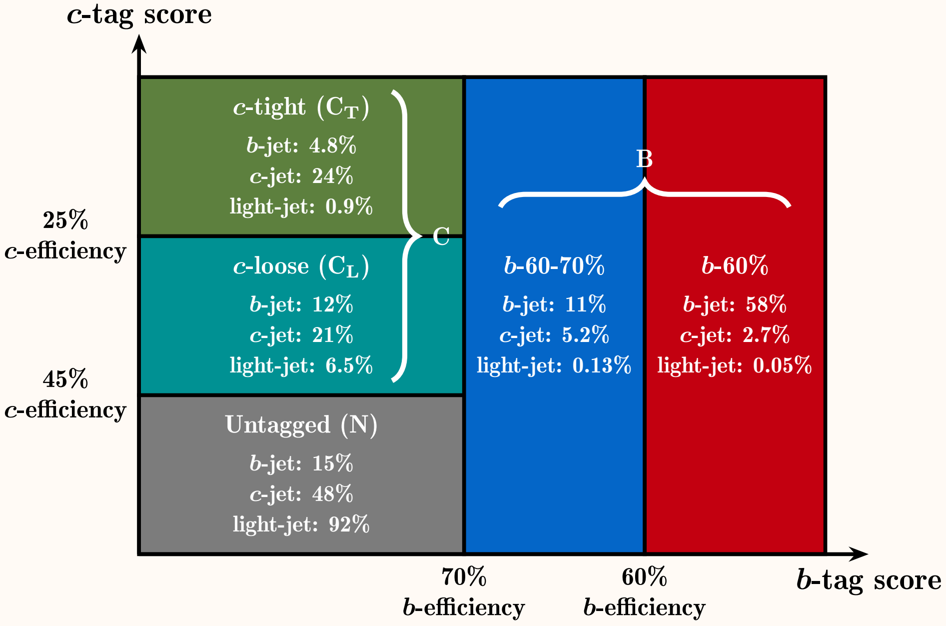

c-tag score

25%
c-efficiency

45%
c-efficiency

c-tight (C_T)
b-jet: 4.8%
c-jet: 24%
light-jet: 0.9%

c-loose (C_L)
b-jet: 12%
c-jet: 21%
light-jet: 6.5%

C

Untagged (N)
b-jet: 15%
c-jet: 48%
light-jet: 92%

B

b-60-70%
b-jet: 11%
c-jet: 5.2%
light-jet: 0.13%

b-60%
b-jet: 58%
c-jet: 2.7%
light-jet: 0.05%

70%
b-efficiency

60%
b-efficiency

b-tag score

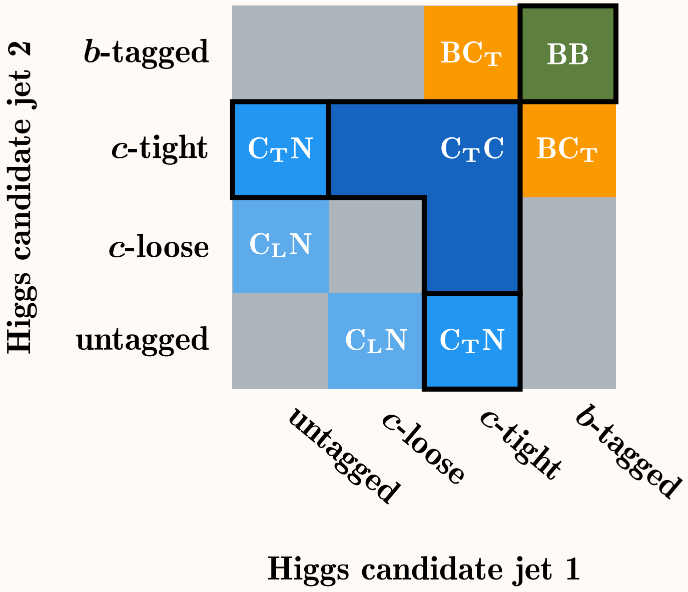

Higgs candidate jet 2

	untagged	*c*-loose	*c*-tight	*b*-tagged
***b*-tagged**			BC_T	BB
***c*-tight**	C_TN		C_TC	BC_T
***c*-loose**	C_LN			
untagged		C_LN	C_TN	

Higgs candidate jet 1

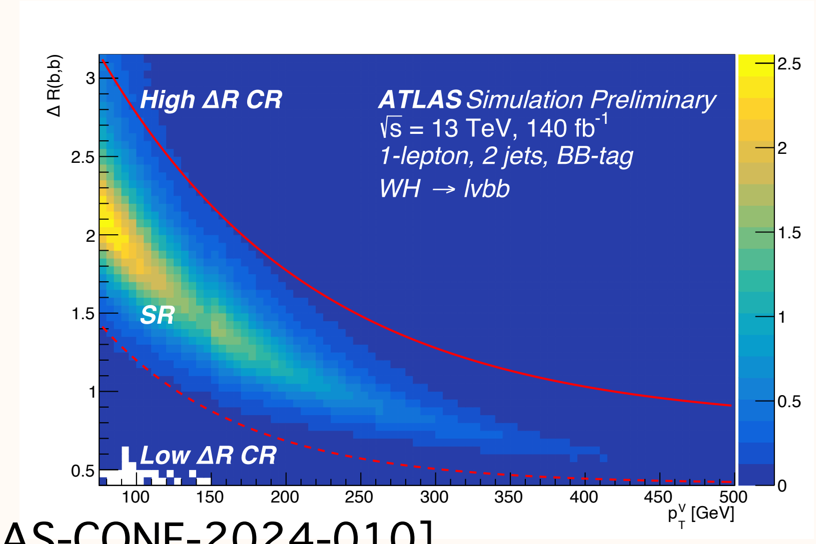

[ATLAS-CONF-2024-010]

Channel	Region	BB	C_TN	C_TC_L	C_TC_T	BC_T	C_LN
0-lepton	High-ΔR CR	Norm. Only				—	
	BC_TTop CR	—				$m_{j_1j_2}$	—
	$V+lf$ CR	—					Norm. Only
1-lepton	Low-ΔR CR	$\text{BDT}_{\text{Low-}\Delta R\,\text{CR}}$	—				
	High-ΔR CR	p_T^V		$m_{j_1j_2}$		—	
	BC_TTop CR	—				$m_{j_1j_2}$	—
	$V+lf$ CR	—					p_T^V
2-lepton	High-ΔR CR	p_T^V		$m_{j_1j_2}$		—	
	Top $e\mu$ CR	—	Norm. Only			–	—
	$V+lf$ CR	—					p_T^V

Constrain on background events

[ATLAS-CONF-2024-010]

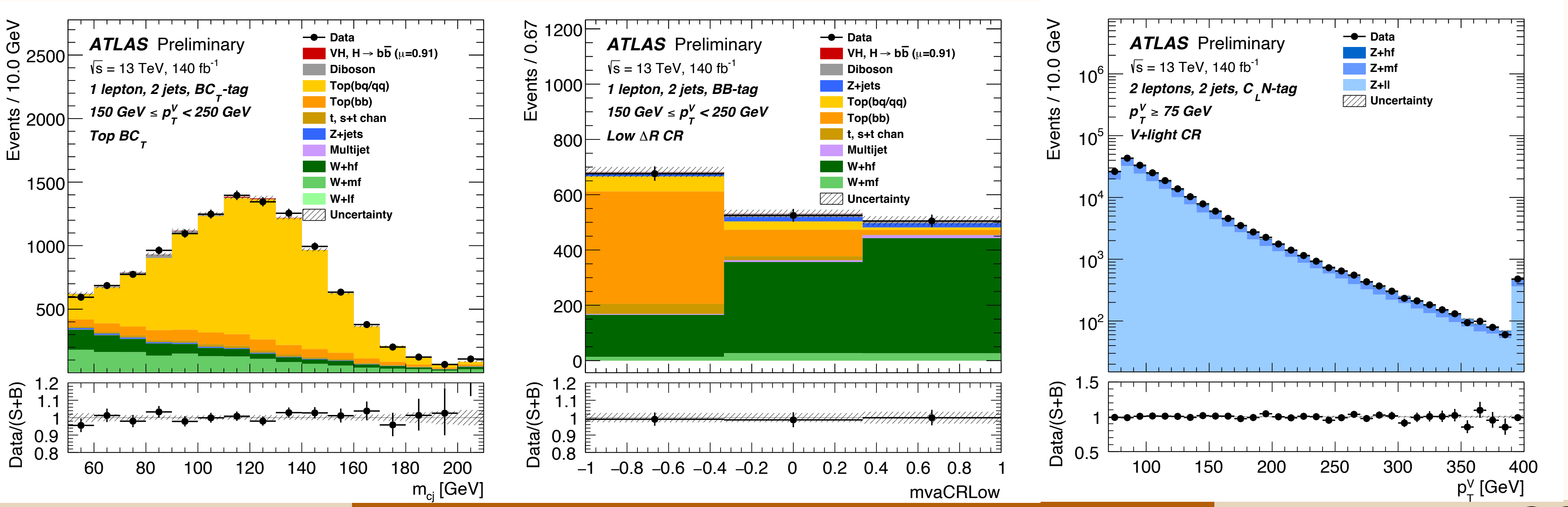

Detailed analysis regions

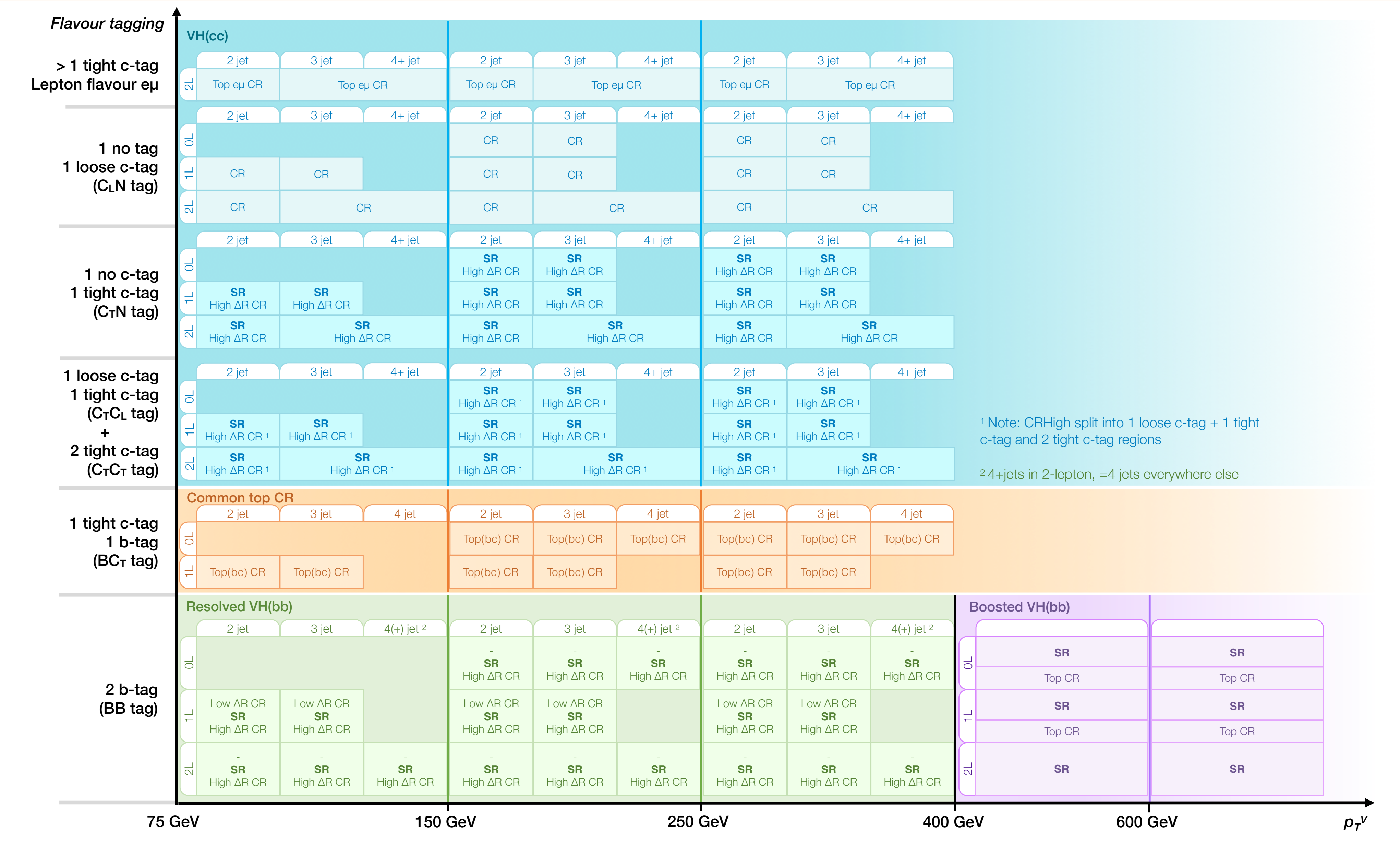

VH(cc)

Flavour tagging		75–150 GeV 2 jet	3 jet	4+ jet	150–250 GeV 2 jet	3 jet	4+ jet	250–400 GeV 2 jet	3 jet	4+ jet
> 1 tight c-tag Lepton flavour eμ	2L	Top eμ CR	Top eμ CR		Top eμ CR	Top eμ CR		Top eμ CR	Top eμ CR	
1 no tag 1 loose c-tag (C$_L$N tag)	0L				CR	CR		CR	CR	
	1L	CR	CR		CR	CR		CR	CR	
	2L	CR	CR		CR	CR		CR	CR	
1 no c-tag 1 tight c-tag (C$_T$N tag)	0L				**SR** High ΔR CR	**SR** High ΔR CR		**SR** High ΔR CR	**SR** High ΔR CR	
	1L	**SR** High ΔR CR	**SR** High ΔR CR		**SR** High ΔR CR	**SR** High ΔR CR		**SR** High ΔR CR	**SR** High ΔR CR	
	2L	**SR** High ΔR CR	**SR** High ΔR CR		**SR** High ΔR CR	**SR** High ΔR CR		**SR** High ΔR CR	**SR** High ΔR CR	
1 loose c-tag 1 tight c-tag (C$_T$C$_L$ tag) + 2 tight c-tag (C$_T$C$_T$ tag)	0L				**SR** High ΔR CR [1]	**SR** High ΔR CR [1]		**SR** High ΔR CR [1]	**SR** High ΔR CR [1]	
	1L	**SR** High ΔR CR [1]	**SR** High ΔR CR [1]		**SR** High ΔR CR [1]	**SR** High ΔR CR [1]		**SR** High ΔR CR [1]	**SR** High ΔR CR [1]	
	2L	**SR** High ΔR CR [1]	**SR** High ΔR CR [1]		**SR** High ΔR CR [1]	**SR** High ΔR CR [1]		**SR** High ΔR CR [1]	**SR** High ΔR CR [1]	

Common top CR

Flavour tagging		75–150 GeV 2 jet	3 jet	4 jet	150–250 GeV 2 jet	3 jet	4 jet	250–400 GeV 2 jet	3 jet	4 jet
1 tight c-tag 1 b-tag (BC$_T$ tag)	0L				Top(bc) CR	Top(bc) CR	Top(bc) CR	Top(bc) CR	Top(bc) CR	Top(bc) CR
	1L	Top(bc) CR	Top(bc) CR		Top(bc) CR	Top(bc) CR		Top(bc) CR	Top(bc) CR	

Resolved VH(bb) / **Boosted VH(bb)**

Flavour tagging		75–150 GeV 2 jet	3 jet	4(+) jet [2]	150–250 GeV 2 jet	3 jet	4(+) jet [2]	250–400 GeV 2 jet	3 jet	4(+) jet [2]	400–600 GeV	600 GeV–
2 b-tag (BB tag)	0L				- **SR** High ΔR CR	- **SR** High ΔR CR	- **SR** High ΔR CR	- **SR** High ΔR CR	- **SR** High ΔR CR	- **SR** High ΔR CR	**SR** Top CR	**SR** Top CR
	1L	Low ΔR CR **SR** High ΔR CR	Low ΔR CR **SR** High ΔR CR		Low ΔR CR **SR** High ΔR CR	Low ΔR CR **SR** High ΔR CR		Low ΔR CR **SR** High ΔR CR	Low ΔR CR **SR** High ΔR CR		**SR** Top CR	**SR** Top CR
	2L	- **SR** High ΔR CR	- **SR** High ΔR CR	- **SR** High ΔR CR	- **SR** High ΔR CR	- **SR** High ΔR CR	- **SR** High ΔR CR	- **SR** High ΔR CR	- **SR** High ΔR CR	- **SR** High ΔR CR	**SR**	**SR**

[1] Note: CRHigh split into 1 loose c-tag + 1 tight c-tag and 2 tight c-tag regions

[2] 4+jets in 2-lepton, =4 jets everywhere else

MC sample list

Process	ME generator	ME PDF	PS and Hadronisation	UE tune	Cross-section order
Signal, mass set to 125 GeV and $b\bar{b}$ branching fraction to 58%					
$qq \to VH$	Powheg Box v2 [53] + GoSam [54]+ MiNLO [65,66]	NNPDF3.0NLO $^{(\star)}$ [55]	Pythia 8.245 [56]	AZNLO [57]	NNLO(QCD)$^{(\dagger)}$+ NLO(EW) [58,59,60,61,62,63,64]
$gg \to ZH$	Powheg Box v2	NNPDF3.0NLO $^{(\star)}$	Pythia 8.245	AZNLO	NLO+ NLL [67,68,69,70,71]
Top quark, mass set to 172.5 GeV					
$t\bar{t}$	Powheg Box v2 [72]	NNPDF3.0NLO	Pythia 8.230	A14 [73]	NNLO+NNLL [74]
s-chan. single top	Powheg Box v2 [75]	NNPDF3.0NLO	Pythia 8.230	A14	NLO [76]
t-chan. single top	Powheg Box v2 [75]	NNPDF3.0NLO	Pythia 8.230	A14	NNLO [77]
Wt	Powheg Box v2 [78]	NNPDF3.0NLO	Pythia 8.230	A14	Approx. NNLO+NNLL [79]
Vector boson + jets					
V+jets	Sherpa 2.2.11 [81,82,83]	NNPDF3.0NNLO	Sherpa 2.2.11 [84,85]	Default	NNLO [80]
Diboson					
$qq \to VV$	Sherpa 2.2.11	NNPDF3.0NNLO	Sherpa 2.2.11	Default	NLO$^{(\ddagger)}$
$gg \to VV$	Sherpa 2.2.2	NNPDF3.0NNLO	Sherpa 2.2.2	Default	NLO$^{(\ddagger)}$

Jet energy correction

[ATLAS-CONF-2024-010]

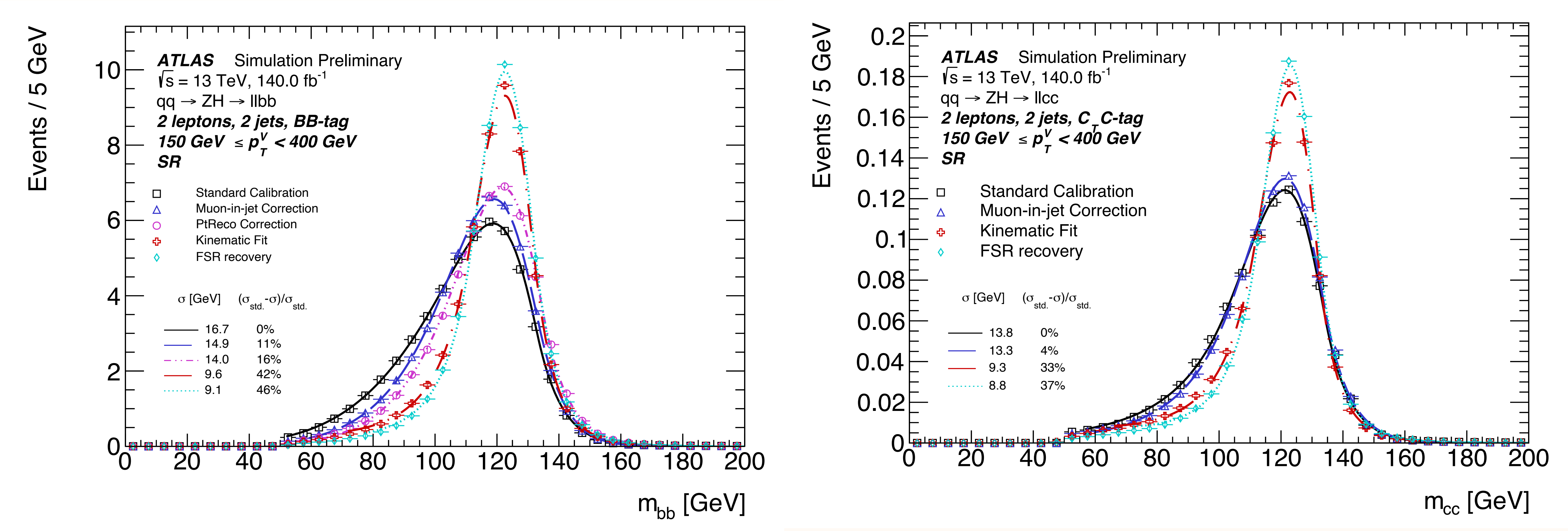

Event migration in STXS measurement

[ATLAS-CONF-2024-010]

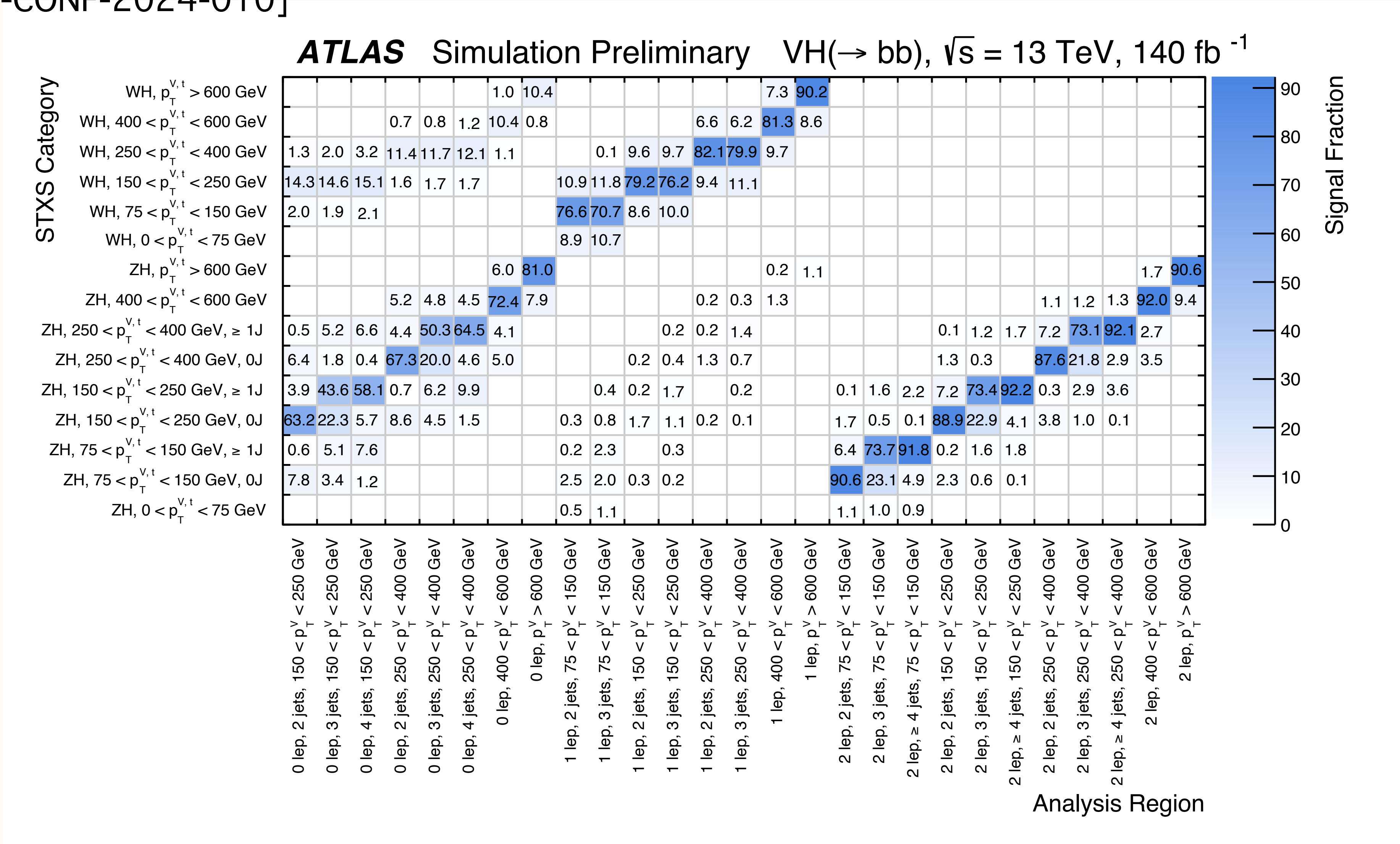

STXS Category	0 lep, 2 jets, 150 < p_T^V < 250 GeV	0 lep, 3 jets, 150 < p_T^V < 250 GeV	0 lep, 4 jets, 150 < p_T^V < 250 GeV	0 lep, 2 jets, 250 < p_T^V < 400 GeV	0 lep, 3 jets, 250 < p_T^V < 400 GeV	0 lep, 4 jets, 250 < p_T^V < 400 GeV	0 lep, 400 < p_T^V < 600 GeV	0 lep, p_T^V > 600 GeV	1 lep, 2 jets, 75 < p_T^V < 150 GeV	1 lep, 3 jets, 75 < p_T^V < 150 GeV	1 lep, 2 jets, 150 < p_T^V < 250 GeV	1 lep, 3 jets, 150 < p_T^V < 250 GeV	1 lep, 2 jets, 250 < p_T^V < 400 GeV	1 lep, 3 jets, 250 < p_T^V < 400 GeV	1 lep, 400 < p_T^V < 600 GeV	1 lep, p_T^V > 600 GeV	2 lep, 2 jets, 75 < p_T^V < 150 GeV	2 lep, 3 jets, 75 < p_T^V < 150 GeV	2 lep, ≥ 4 jets, 75 < p_T^V < 150 GeV	2 lep, 2 jets, 150 < p_T^V < 250 GeV	2 lep, 3 jets, 150 < p_T^V < 250 GeV	2 lep, ≥ 4 jets, 150 < p_T^V < 250 GeV	2 lep, 2 jets, 250 < p_T^V < 400 GeV	2 lep, 3 jets, 250 < p_T^V < 400 GeV	2 lep, ≥ 4 jets, 250 < p_T^V < 400 GeV	2 lep, 400 < p_T^V < 600 GeV	2 lep, p_T^V > 600 GeV
WH, $p_T^{V,t}$ > 600 GeV							1.0	10.4							7.3	90.2											
WH, 400 < $p_T^{V,t}$ < 600 GeV				0.7	0.8	1.2	10.4	0.8					6.6	6.2	81.3	8.6											
WH, 250 < $p_T^{V,t}$ < 400 GeV	1.3	2.0	3.2	11.4	11.7	12.1	1.1			0.1	9.6	9.7	82.1	79.9	9.7												
WH, 150 < $p_T^{V,t}$ < 250 GeV	14.3	14.6	15.1	1.6	1.7	1.7			10.9	11.8	79.2	76.2	9.4	11.1													
WH, 75 < $p_T^{V,t}$ < 150 GeV	2.0	1.9	2.1						76.6	70.7	8.6	10.0															
WH, 0 < $p_T^{V,t}$ < 75 GeV									8.9	10.7																	
ZH, $p_T^{V,t}$ > 600 GeV							6.0	81.0							0.2	1.1										1.7	90.6
ZH, 400 < $p_T^{V,t}$ < 600 GeV				5.2	4.8	4.5	72.4	7.9					0.2	0.3	1.3								1.1	1.2	1.3	92.0	9.4
ZH, 250 < $p_T^{V,t}$ < 400 GeV, ≥ 1J	0.5	5.2	6.6	4.4	50.3	64.5	4.1					0.2	0.2	1.4						0.1	1.2	1.7	7.2	73.1	92.1	2.7	
ZH, 250 < $p_T^{V,t}$ < 400 GeV, 0J	6.4	1.8	0.4	67.3	20.0	4.6	5.0				0.2	0.4	1.3	0.7						1.3	0.3		87.6	21.8	2.9	3.5	
ZH, 150 < $p_T^{V,t}$ < 250 GeV, ≥ 1J	3.9	43.6	58.1	0.7	6.2	9.9				0.4	0.2	1.7		0.2			0.1	1.6	2.2	7.2	73.4	92.2	0.3	2.9	3.6		
ZH, 150 < $p_T^{V,t}$ < 250 GeV, 0J	63.2	22.3	5.7	8.6	4.5	1.5			0.3	0.8	1.7	1.1	0.2	0.1			1.7	0.5	0.1	88.9	22.9	4.1	3.8	1.0	0.1		
ZH, 75 < $p_T^{V,t}$ < 150 GeV, ≥ 1J	0.6	5.1	7.6						0.2	2.3		0.3					6.4	73.7	91.8	0.2	1.6	1.8					
ZH, 75 < $p_T^{V,t}$ < 150 GeV, 0J	7.8	3.4	1.2						2.5	2.0	0.3	0.2					90.6	23.1	4.9	2.3	0.6	0.1					
ZH, 0 < $p_T^{V,t}$ < 75 GeV									0.5	1.1							1.1	1.0	0.9								

Background fraction in every analysis region

[ATLAS-CONF-2024-010]

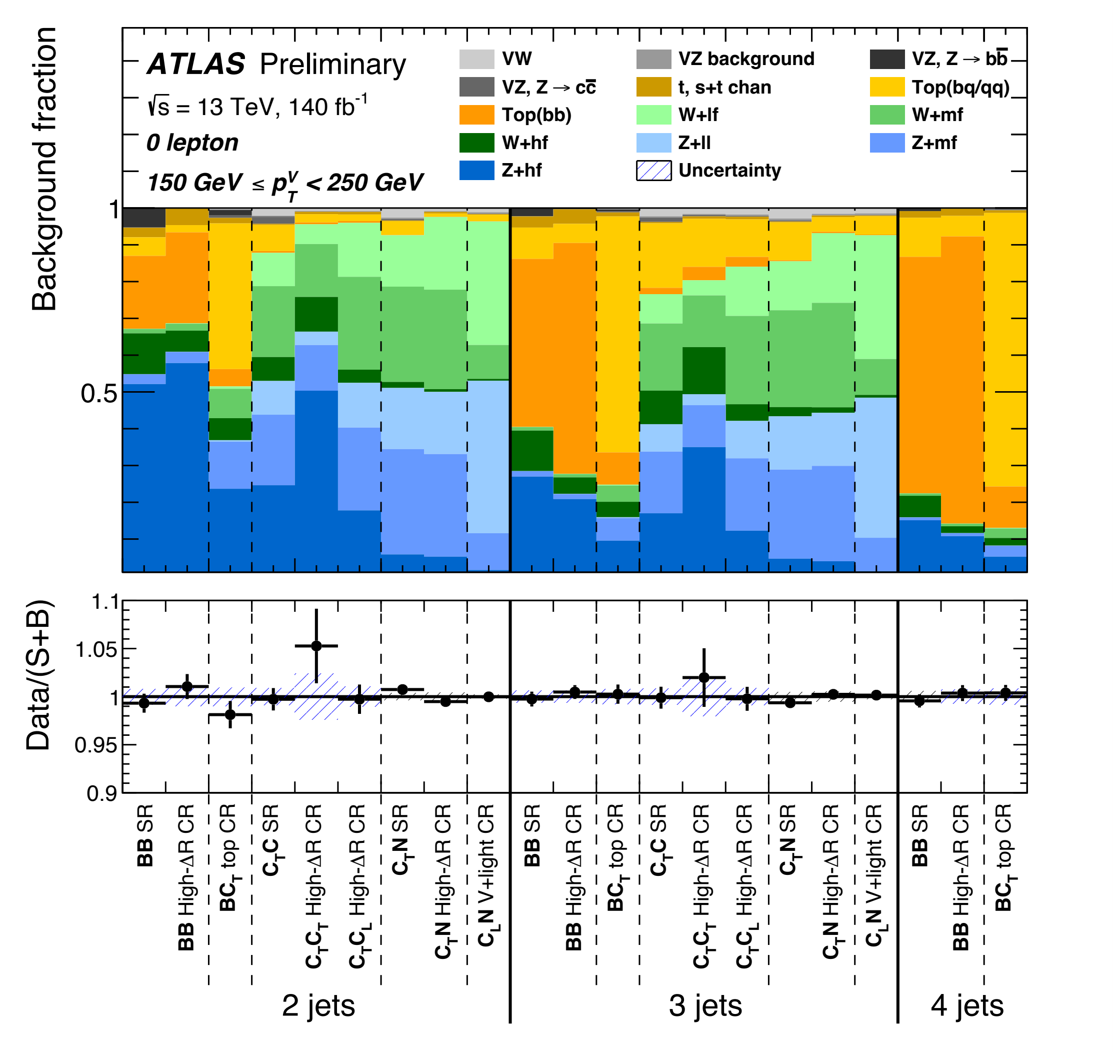

0-lepton, Resolved VH,H→bb,cc

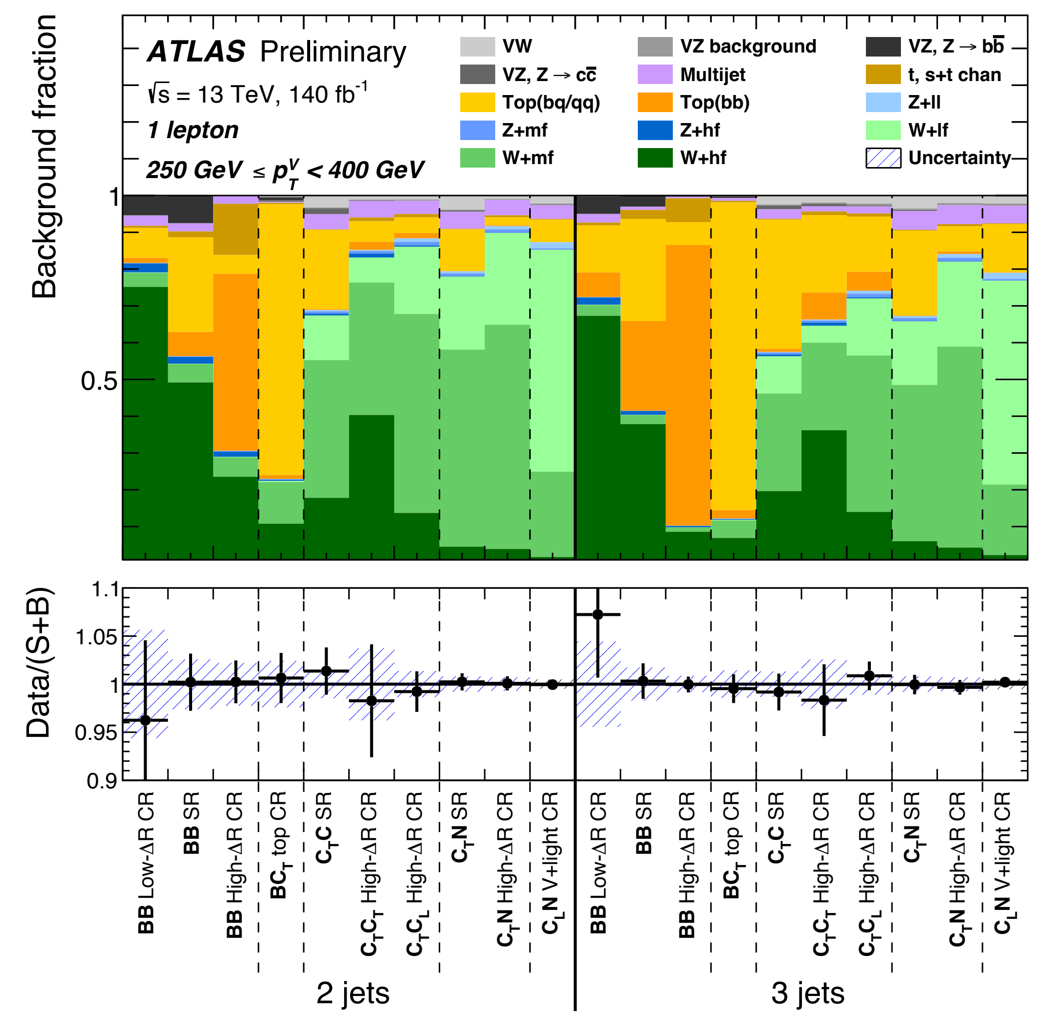

1-lepton, Resolved VH,H→bb,cc

Background fraction in every analysis region

[ATLAS-CONF-2024-010]

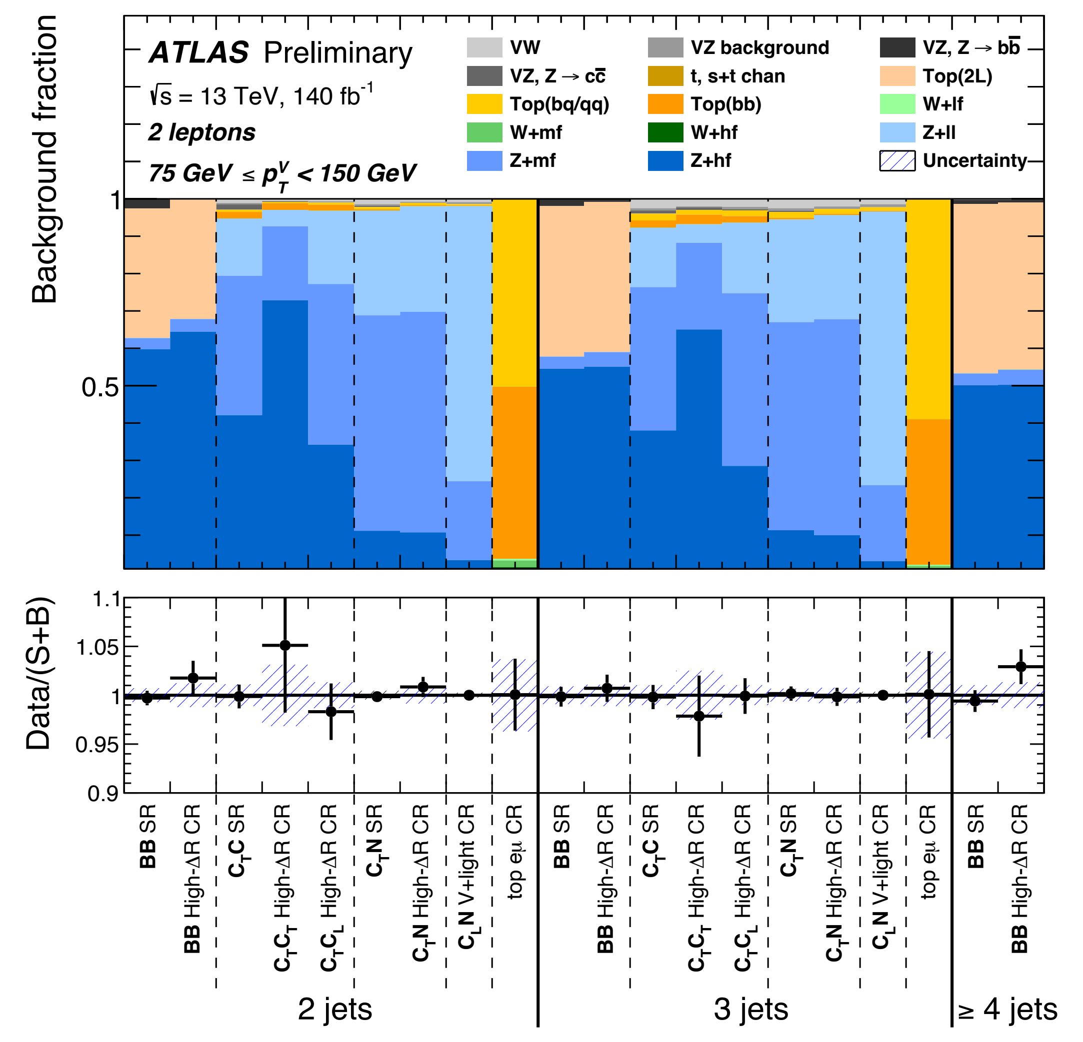

2-lepton, Resolved VH,H→bb,cc

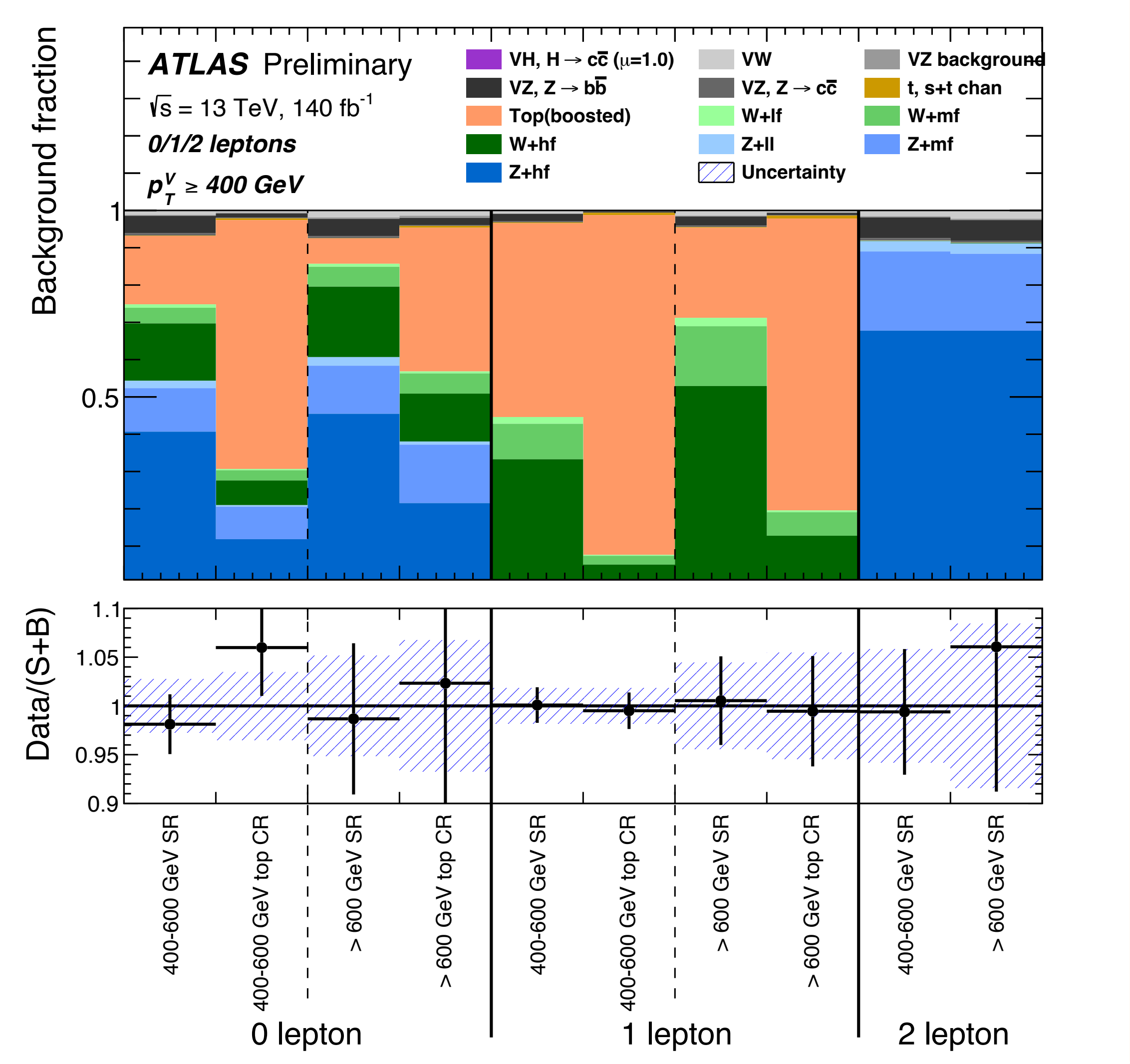

Boosted VH,H→bb

Input variables for the MVA final discriminant variable

	Resolved$_{0}$ $VH, H \to b\bar{b}, c\bar{c}$			Boosted$_{0}$ $VH, H \to b\bar{b}$		
Variable	0-lepton	1-lepton	2-lepton	0-lepton	1-lepton	2-lepton
m_H	✓	✓	✓	✓	✓	✓
$m_{j_1 j_2 j_3}$	✓	✓	✓			
$p_{\mathrm{T}}^{j_1}$	✓	✓	✓	✓	✓	✓
$p_{\mathrm{T}}^{j_2}$	✓	✓	✓	✓	✓	✓
$p_{\mathrm{T}}^{j_3}$				✓	✓	✓
$\sum p_{\mathrm{T}}^{j_i}$, $i > 2$	✓	✓	✓			
$\mathrm{bin}_{D_{\mathrm{DL1r}}}(j_1)$	✓	✓	✓	✓	✓	✓
$\mathrm{bin}_{D_{\mathrm{DL1r}}}(j_2)$	✓	✓	✓	✓	✓	✓
p_{T}^{V}	$\equiv E_{\mathrm{T}}^{\mathrm{miss}}$	✓	✓	$\equiv E_{\mathrm{T}}^{\mathrm{miss}}$	✓	✓
$E_{\mathrm{T}}^{\mathrm{miss}}$	✓	✓		✓	✓	
$E_{\mathrm{T}}^{\mathrm{miss}}/\sqrt{S_{\mathrm{T}}}$			✓			
$\lvert\Delta\phi(\vec{V}, \vec{H})\rvert$	✓	✓	✓	✓	✓	✓
$\lvert\Delta y(\vec{V}, \vec{H})\rvert$		✓	✓		✓	✓
$\Delta R(\vec{j_1}, \vec{j_2})$	✓	✓	✓	✓	✓	✓
$\min[\Delta R(\vec{j_i}, \vec{j_1} \text{ or } \vec{j_2})]$, $i > 2$	✓	✓				
N(track-jets in J)				✓	✓	✓
N(add. small R-jets)				✓	✓	✓
colour ring				✓	✓	✓
$\lvert\Delta\eta(\vec{j_1}, \vec{j_2})\rvert$	✓					
$H_{\mathrm{T}} + E_{\mathrm{T}}^{\mathrm{miss}}$	✓					
m_{T}^{W}		✓				
m_{top}		✓				
$\min[\Delta\phi(\vec{\ell}, \vec{j_1} \text{ or } \vec{j_2})]$		✓				
p_{T}^{ℓ}					✓	
$(p_{\mathrm{T}}^{\ell} - E_{\mathrm{T}}^{\mathrm{miss}})/p_{\mathrm{T}}^{V}$					✓	
$m_{\ell\ell}$			✓			
$\cos\theta^{*}(\vec{\ell^{-}}, \vec{V})$			✓			✓

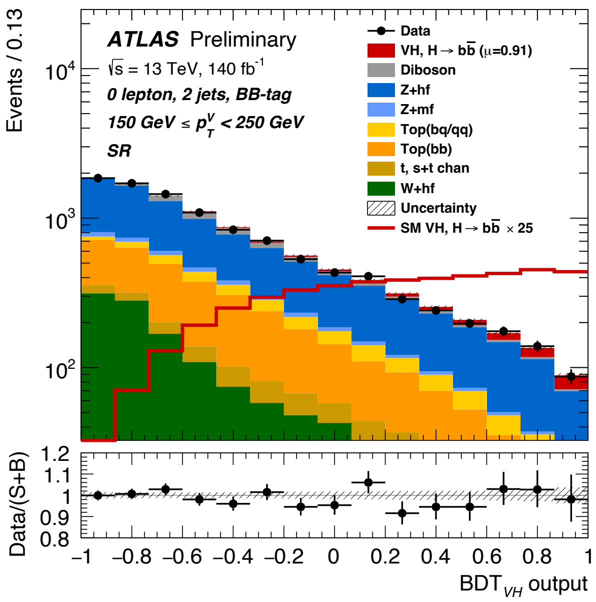

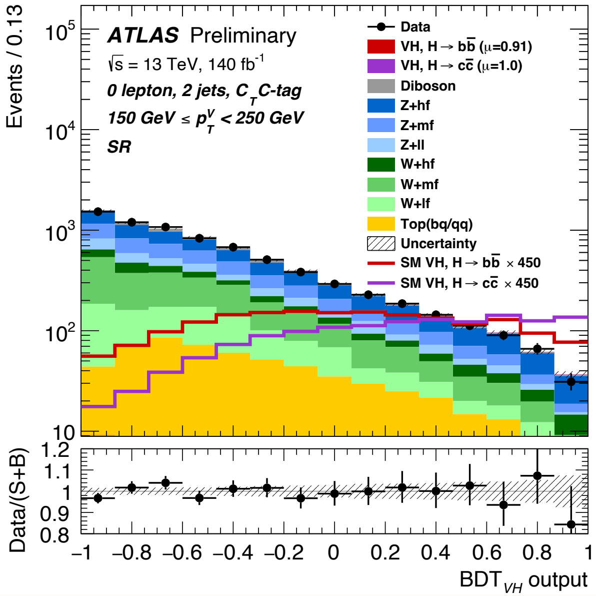

Diboson cross-check fit results

[ATLAS-CONF-2024-010]

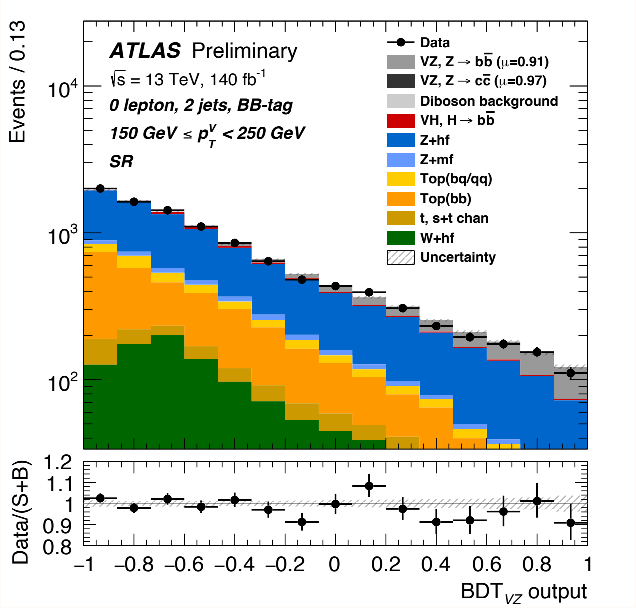

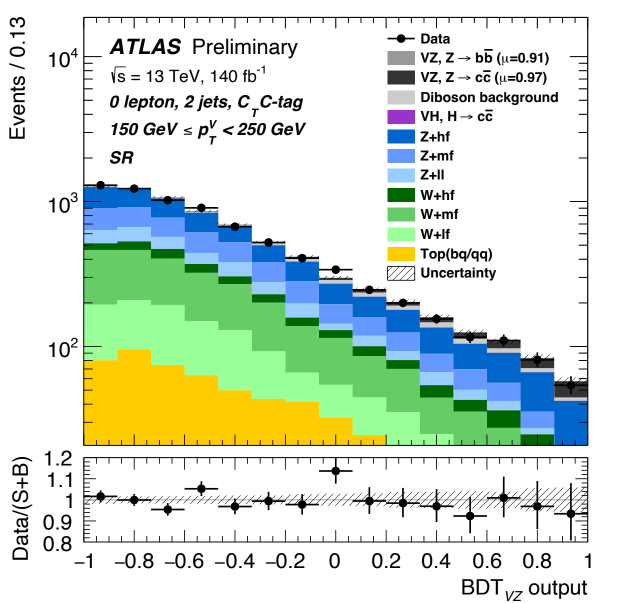

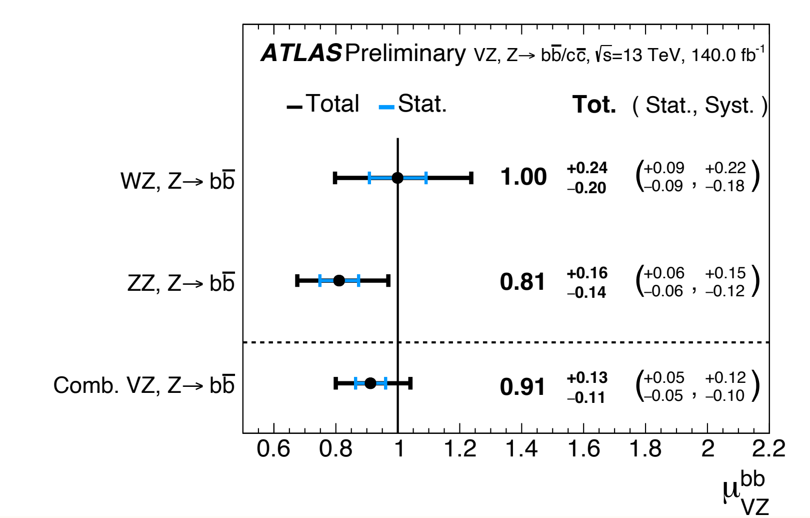

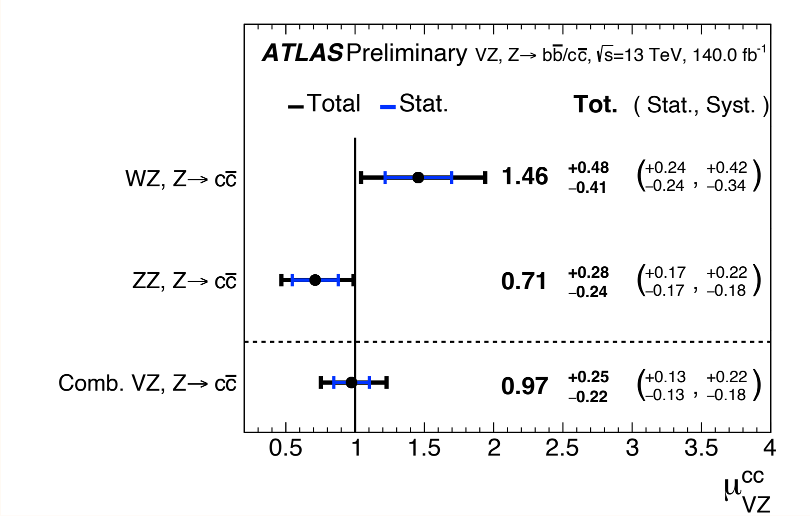

Diboson MVA post-fit plots

[ATLAS-CONF-2024-010]

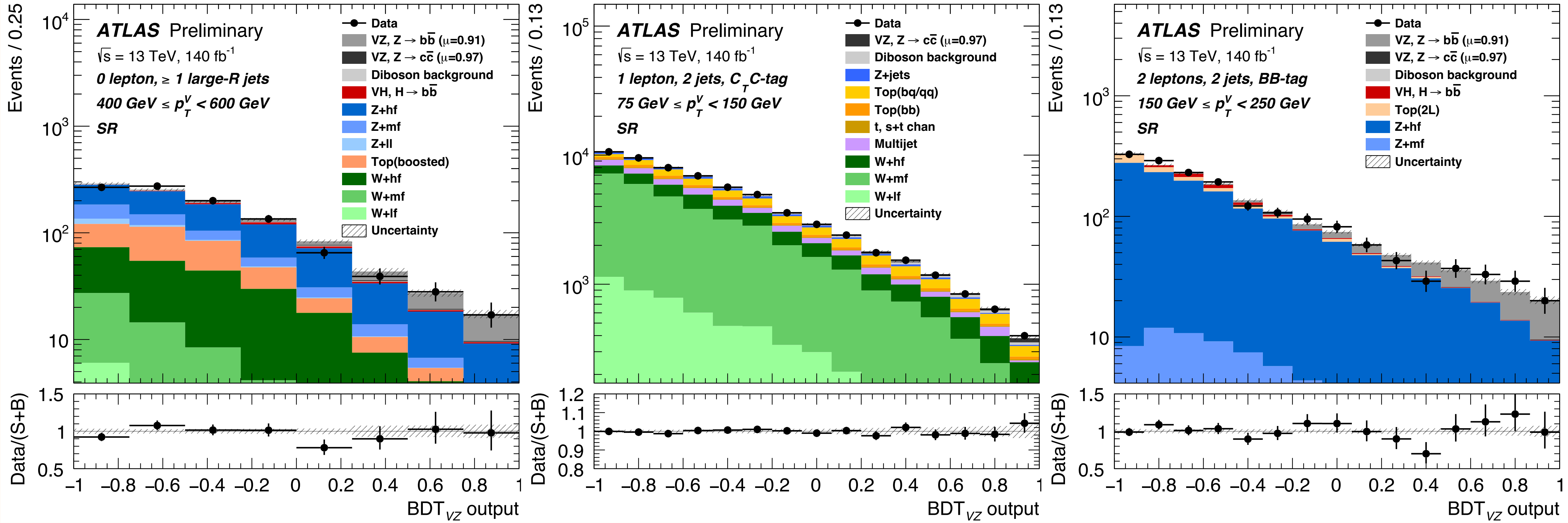

MVA Post-fit plots – Resolved VHbb

[ATLAS-CONF-2024-010]

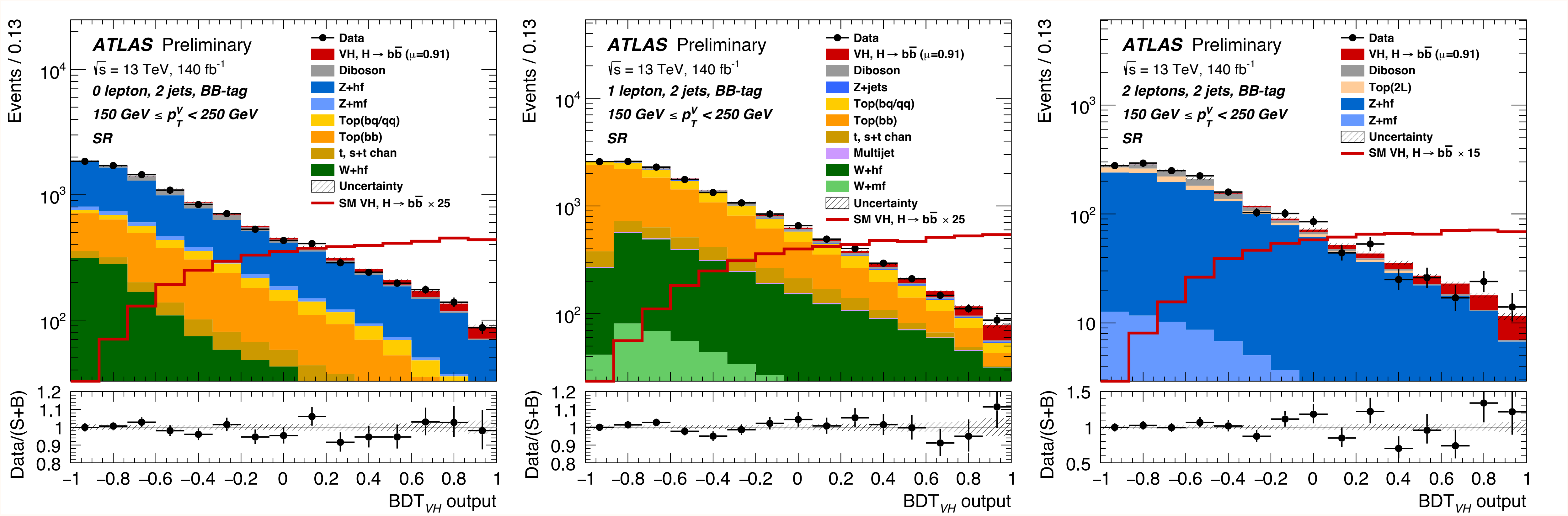

0-lepton

1-lepton

2-lepton

MVA Post-fit plots – Boosted VHbb

[ATLAS-CONF-2024-010]

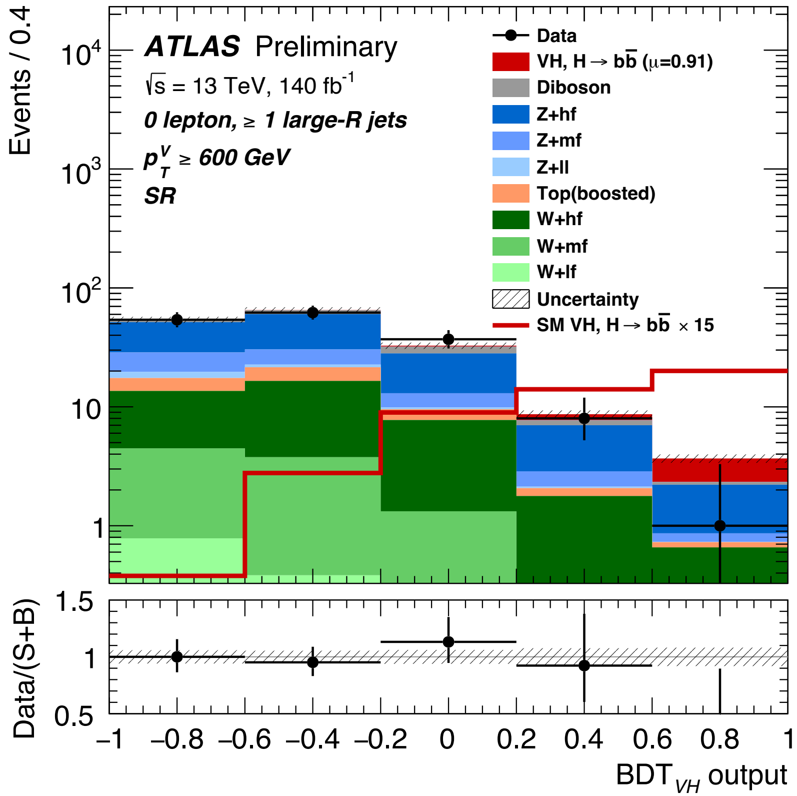

0-lepton

ZH, 600 GeV <pTV

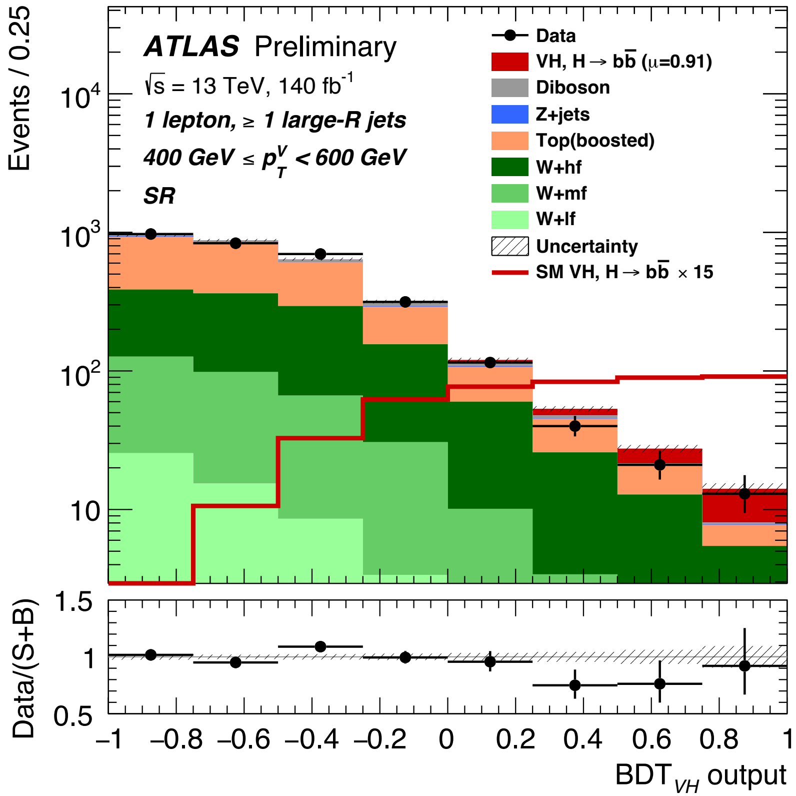

1-lepton

WH, 400<pTV<600 GeV

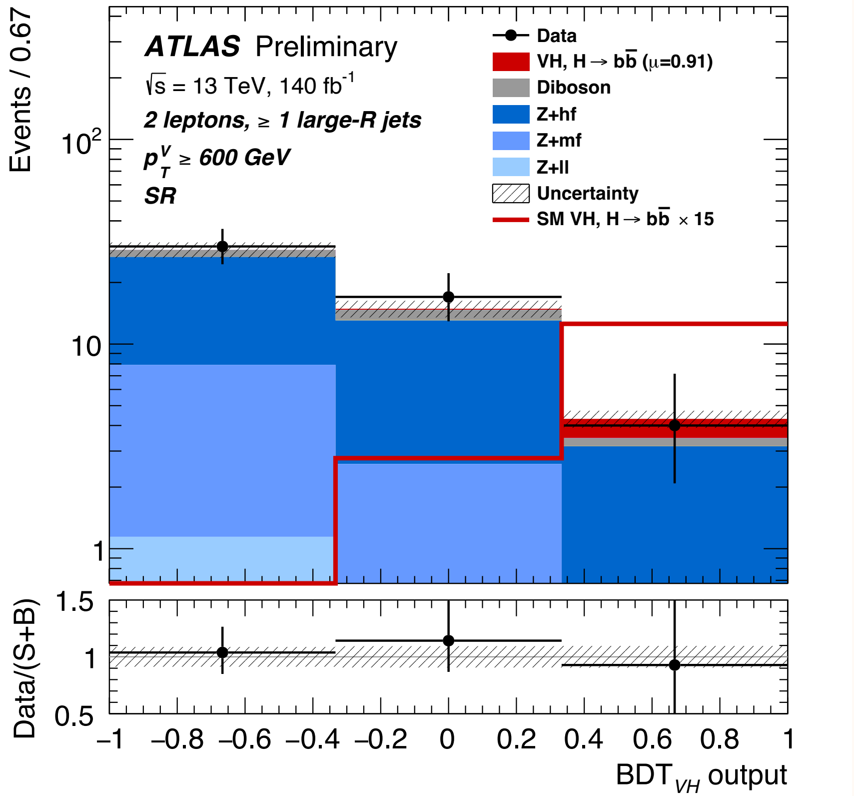

2-lepton

ZH, 600 GeV <pTV

MVA Post-fit plots - VHcc

[ATLAS-CONF-2024-010]

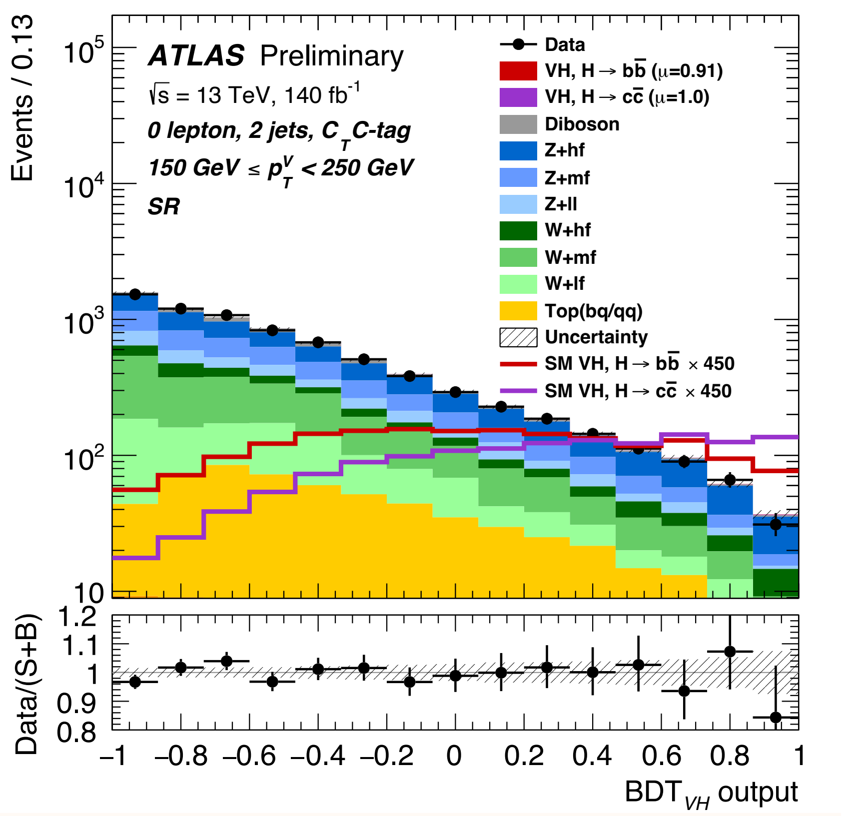

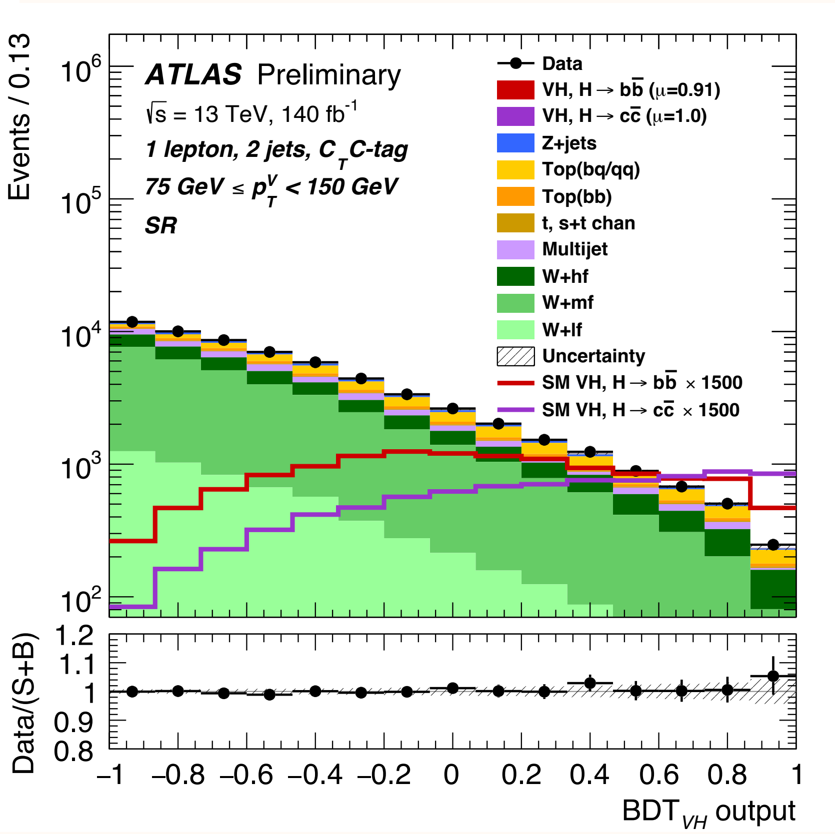

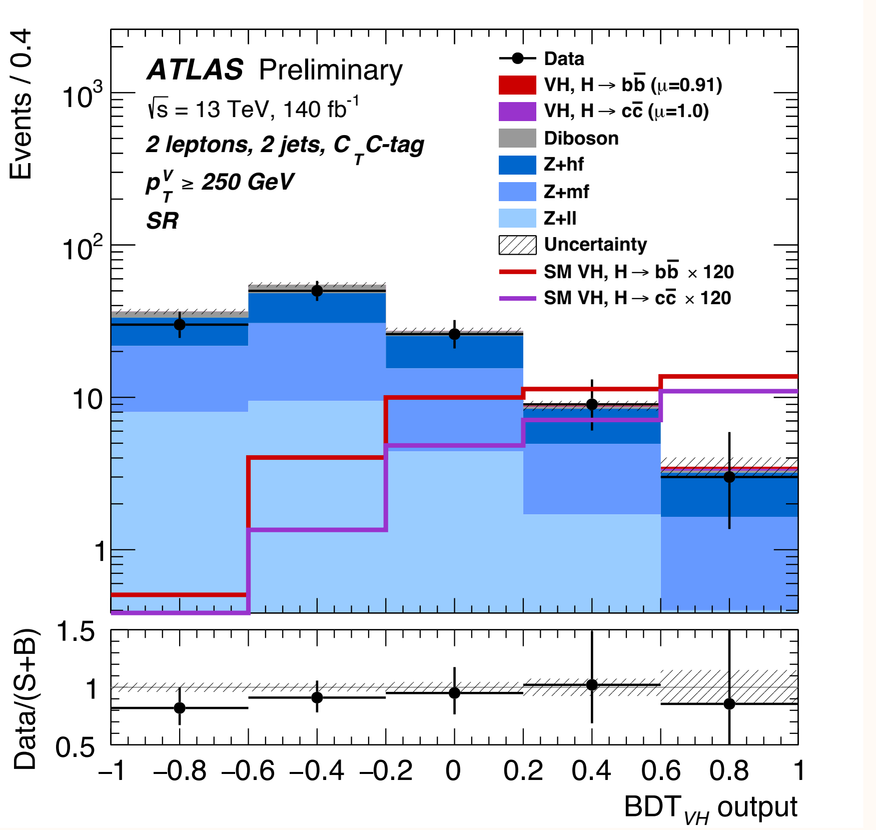

VHbb mu (Comb & WH & ZH)

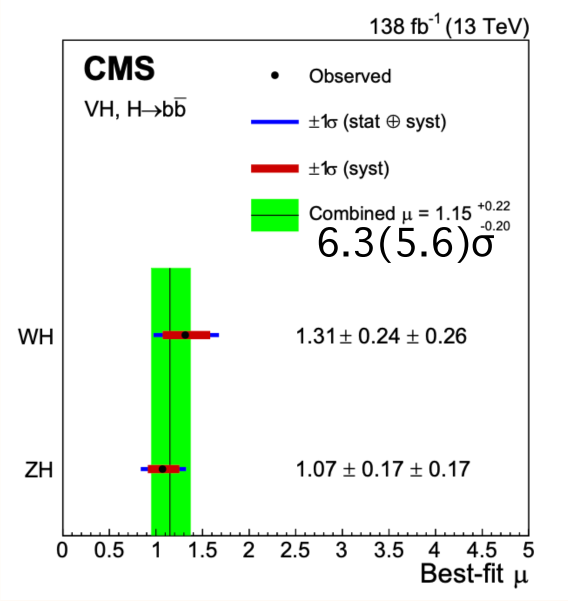

6.3(5.6)σ

Latest CMS result

[Phys. Rev. D 109 (2024) 092011]

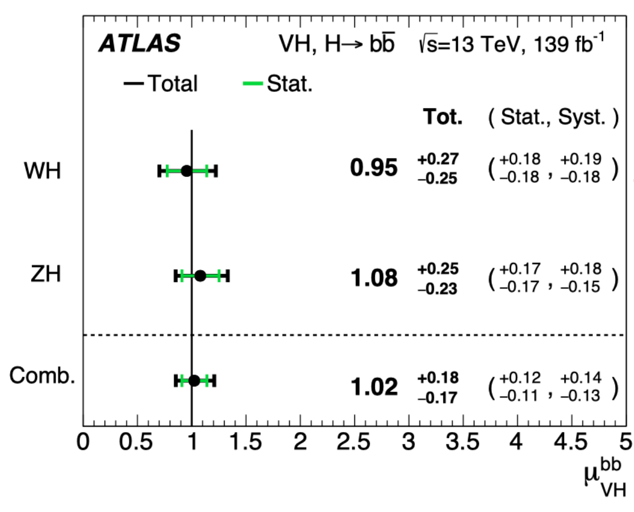

4.0σ

5.3σ

6.7σ
(6.7)

Last ATLAS VH->bb resolved

[Eur. Phys. J. C 81 (2021) 178]

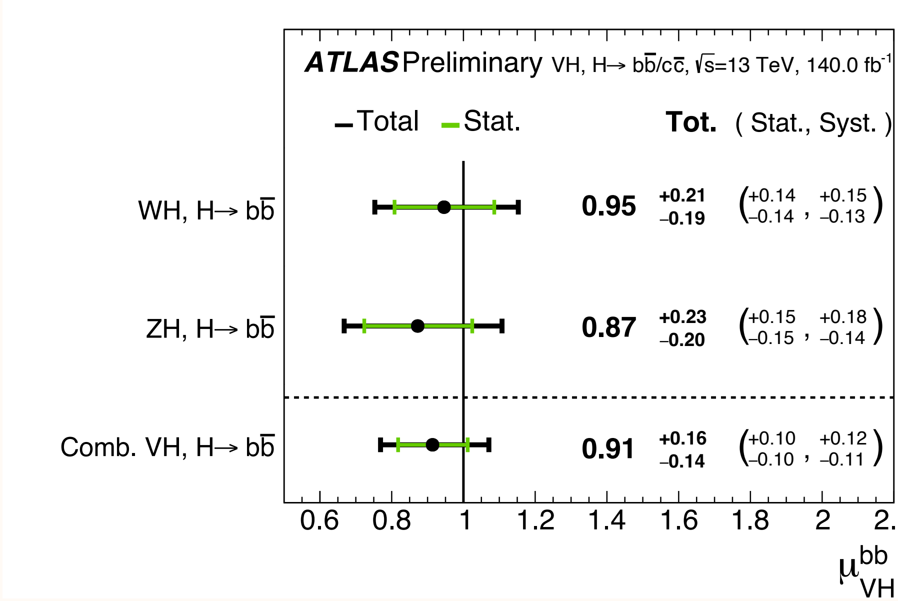

5.3(5.5)σ

4.9(5.7)σ

7.4(8.0)σ

This analysis

[ATLAS-CONF-2024-010]

Last ATLAS VH->bb resolved+boosted

[ATLAS-CONF-2021-051]

μ(VHbb) = 1.00 +0.18 −0.17   6.4(6.3)σ

VHbb and VHcc

[ATLAS-CONF-2024-010]

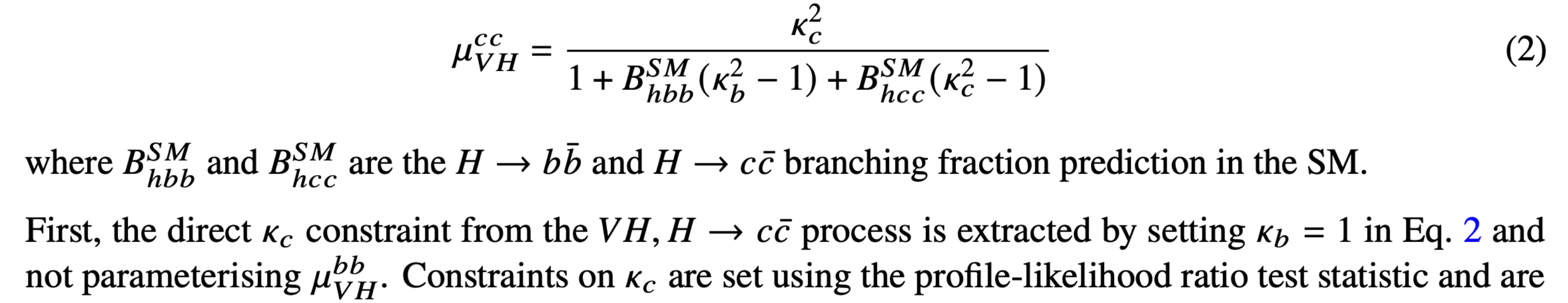

$$\mu_{VH}^{cc} = \frac{\kappa_c^2}{1 + B_{hbb}^{SM}(\kappa_b^2 - 1) + B_{hcc}^{SM}(\kappa_c^2 - 1)} \quad (2)$$

where B_{hbb}^{SM} and B_{hcc}^{SM} are the $H \to b\bar{b}$ and $H \to c\bar{c}$ branching fraction prediction in the SM.

First, the direct κ_c constraint from the $VH, H \to c\bar{c}$ process is extracted by setting $\kappa_b = 1$ in Eq. 2 and not parameterising μ_{VH}^{bb}. Constraints on κ_c are set using the profile-likelihood ratio test statistic and are

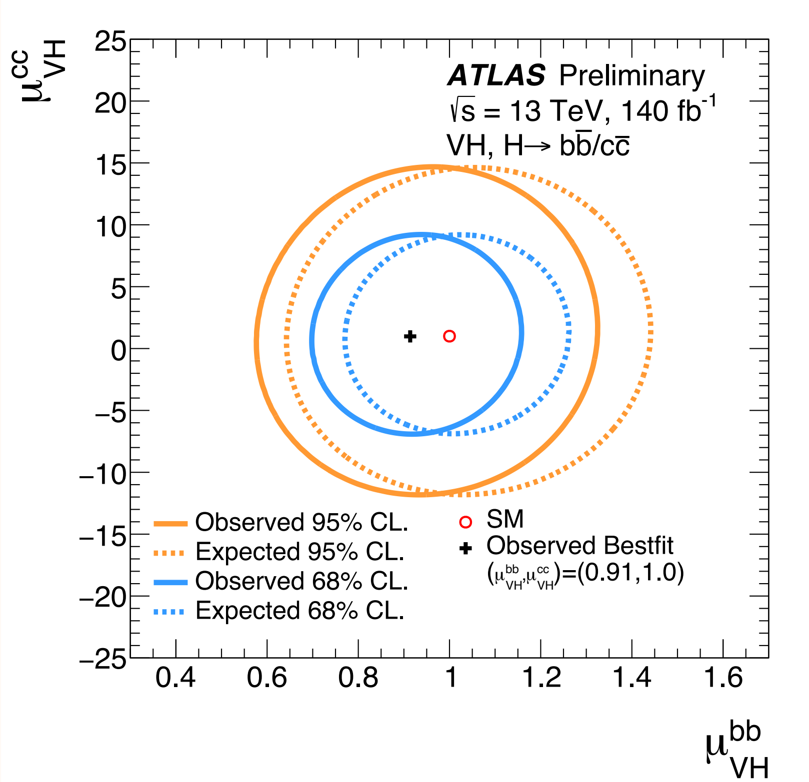

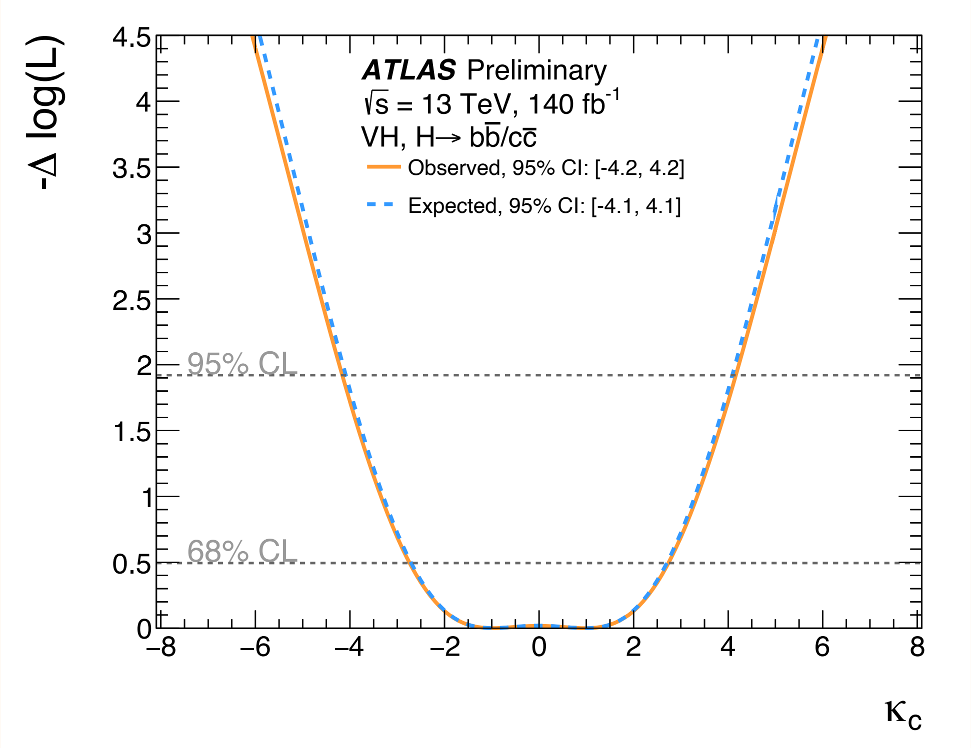

VHcc mu and limit

[Phys. Rev. Lett. 131 (2023) 061801]

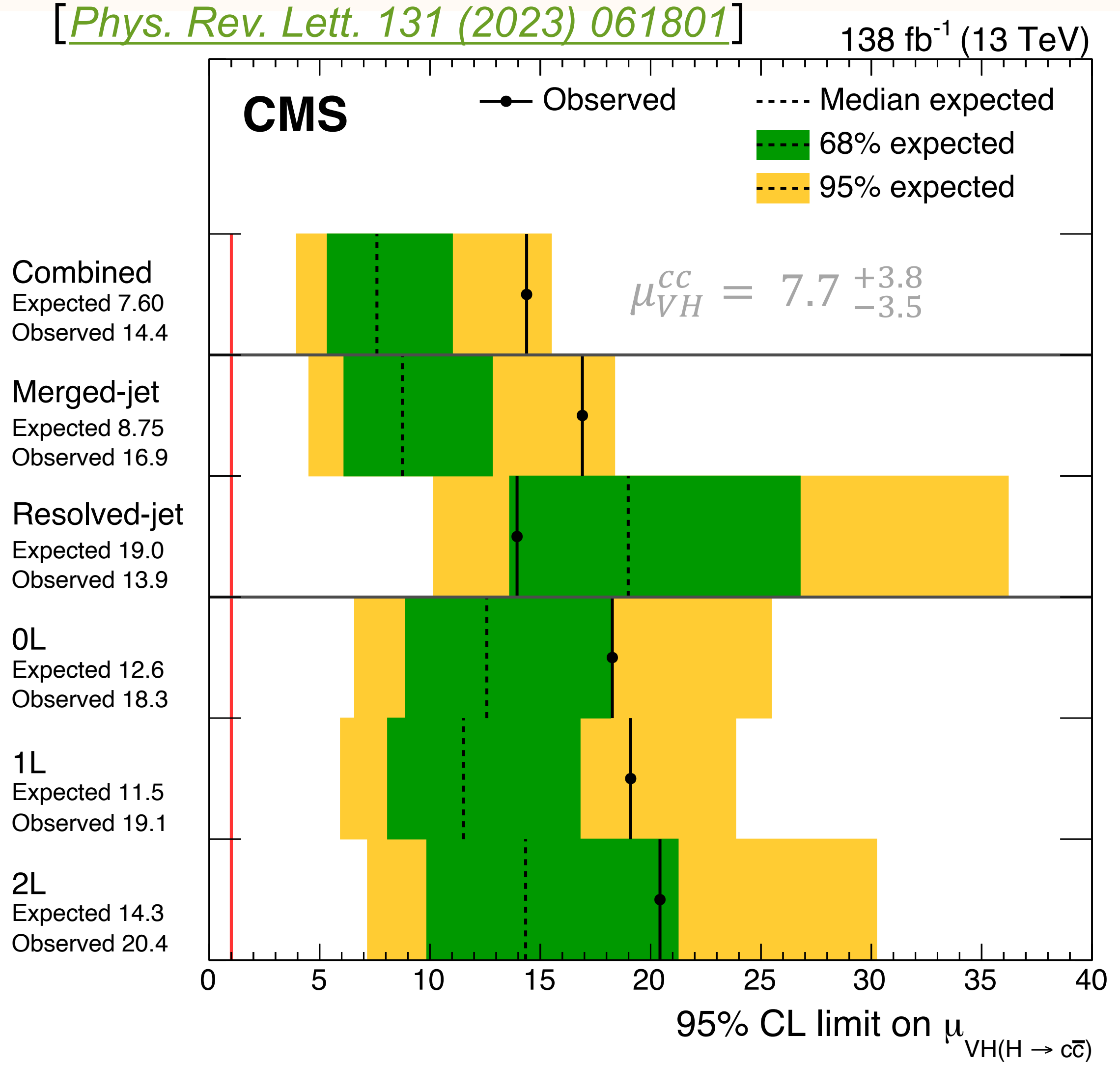

[ATLAS-CONF-2024-010]

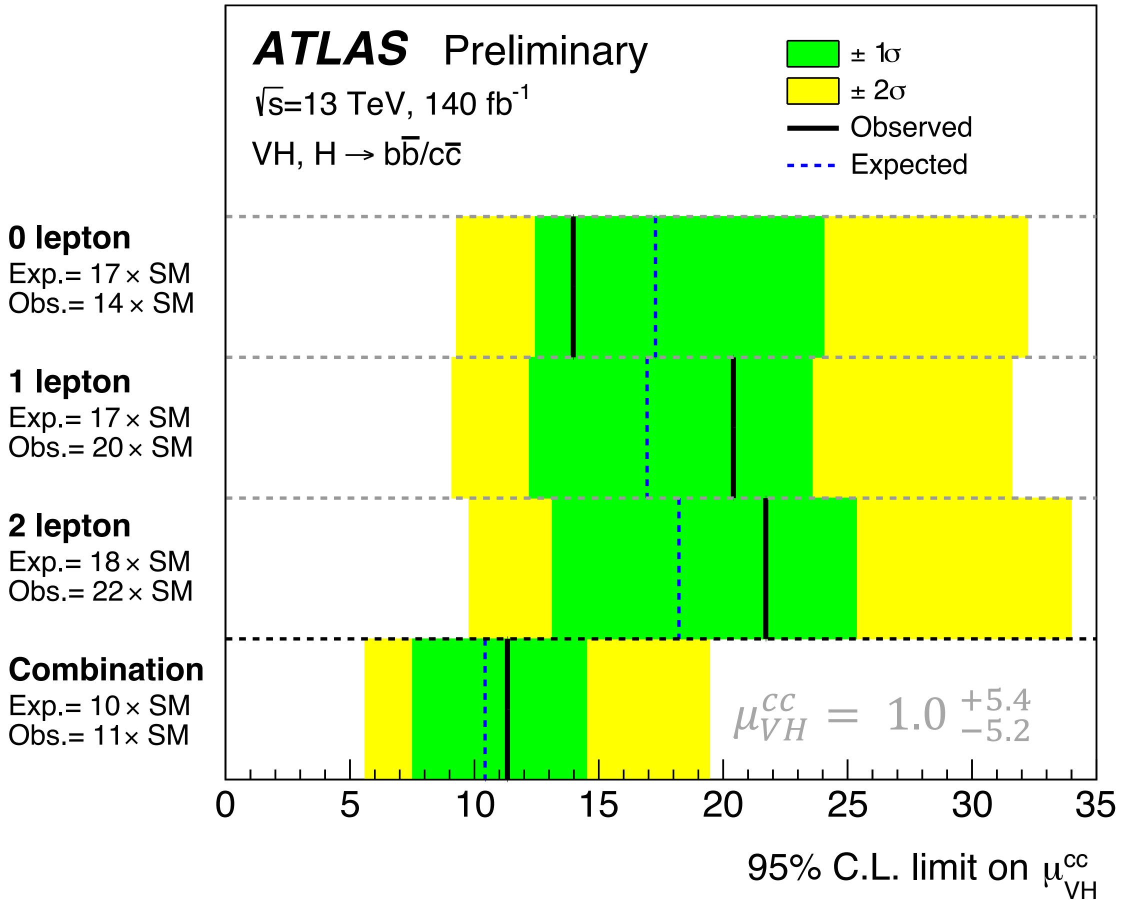

Breakdown table of μ uncertainty

CMS VHbb

[Phys. Rev. D 109 (2024) 092011]

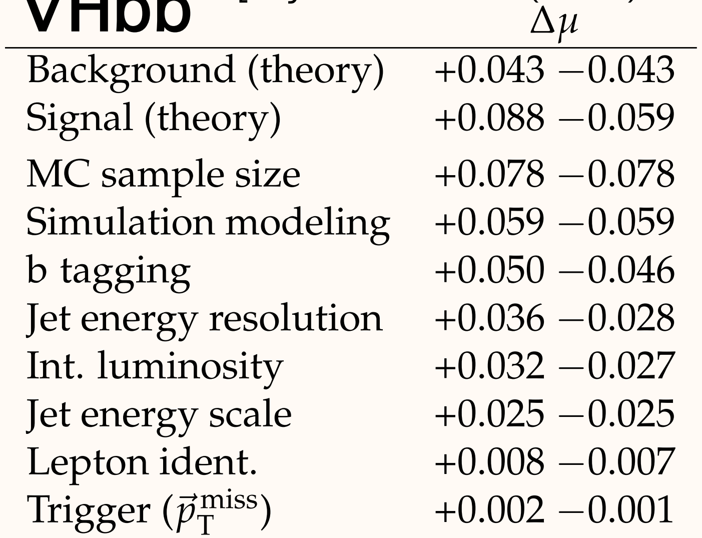

	$\Delta\mu$	
Background (theory)	+0.043	−0.043
Signal (theory)	+0.088	−0.059
MC sample size	+0.078	−0.078
Simulation modeling	+0.059	−0.059
b tagging	+0.050	−0.046
Jet energy resolution	+0.036	−0.028
Int. luminosity	+0.032	−0.027
Jet energy scale	+0.025	−0.025
Lepton ident.	+0.008	−0.007
Trigger ($\vec{p}_{\mathrm{T}}^{\mathrm{miss}}$)	+0.002	−0.001

CMS VHcc

[*Phys. Rev. Lett. 131 (2023) 061801*]

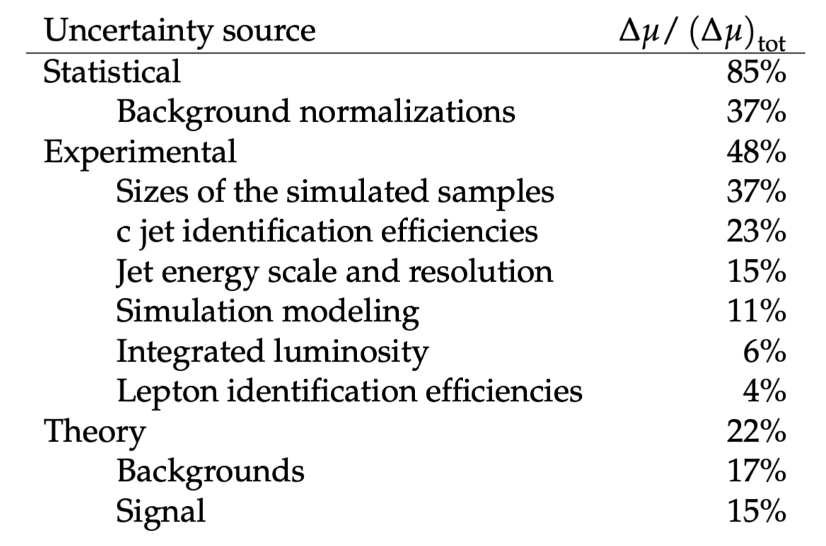

Uncertainty source	$\Delta\mu / (\Delta\mu)_{\mathrm{tot}}$
Statistical	85%
Background normalizations	37%
Experimental	48%
Sizes of the simulated samples	37%
c jet identification efficiencies	23%
Jet energy scale and resolution	15%
Simulation modeling	11%
Integrated luminosity	6%
Lepton identification efficiencies	4%
Theory	22%
Backgrounds	17%
Signal	15%

ATLAS

[ATLAS-CONF-2024-010]

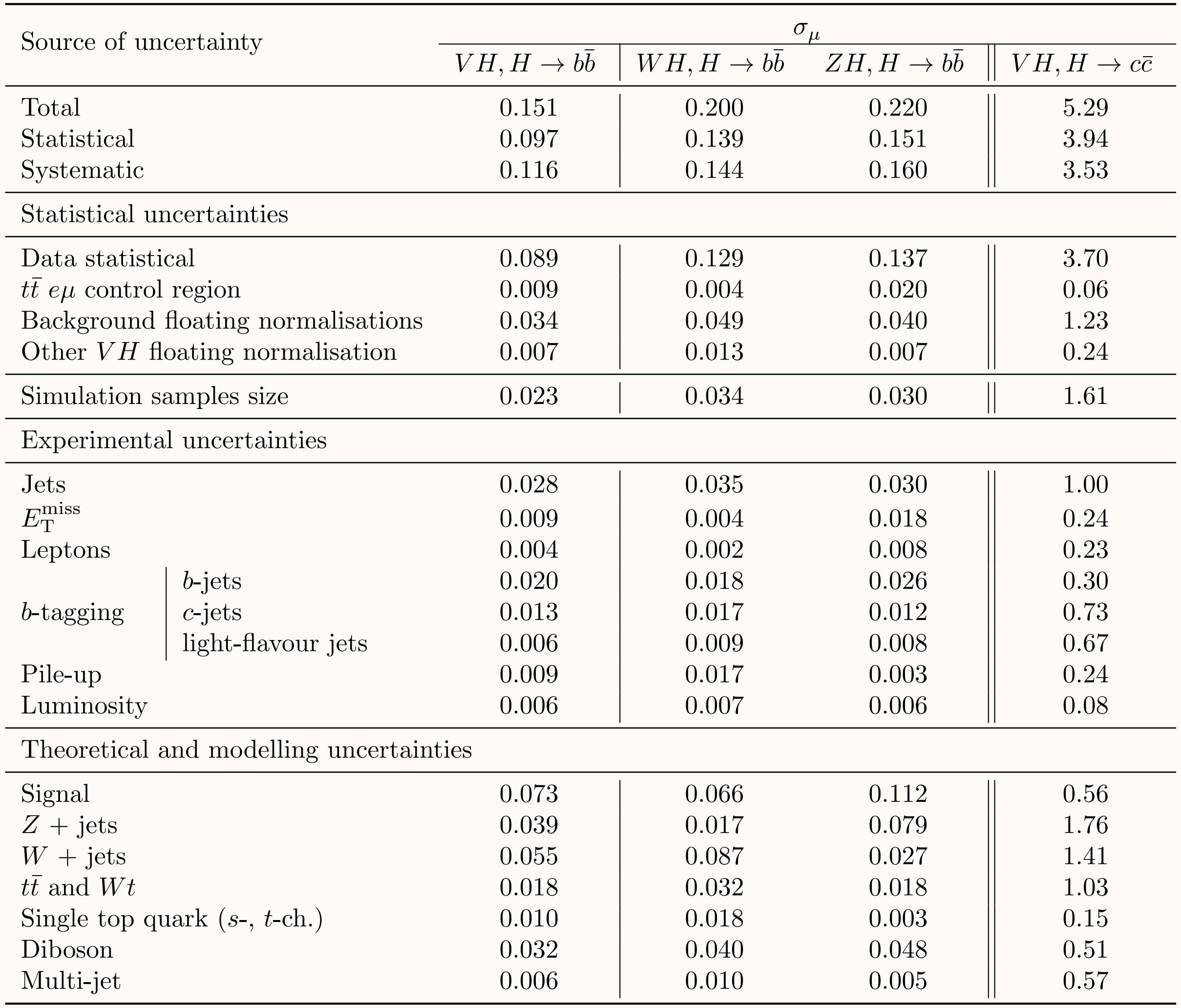

Source of uncertainty		σ_μ		
	$VH, H \to b\bar{b}$	$WH, H \to b\bar{b}$	$ZH, H \to b\bar{b}$	$VH, H \to c\bar{c}$
Total	0.151	0.200	0.220	5.29
Statistical	0.097	0.139	0.151	3.94
Systematic	0.116	0.144	0.160	3.53
Statistical uncertainties				
Data statistical	0.089	0.129	0.137	3.70
$t\bar{t}$ $e\mu$ control region	0.009	0.004	0.020	0.06
Background floating normalisations	0.034	0.049	0.040	1.23
Other VH floating normalisation	0.007	0.013	0.007	0.24
Simulation samples size	0.023	0.034	0.030	1.61
Experimental uncertainties				
Jets	0.028	0.035	0.030	1.00
$E_{\mathrm{T}}^{\mathrm{miss}}$	0.009	0.004	0.018	0.24
Leptons	0.004	0.002	0.008	0.23
b-tagging: b-jets	0.020	0.018	0.026	0.30
b-tagging: c-jets	0.013	0.017	0.012	0.73
b-tagging: light-flavour jets	0.006	0.009	0.008	0.67
Pile-up	0.009	0.017	0.003	0.24
Luminosity	0.006	0.007	0.006	0.08
Theoretical and modelling uncertainties				
Signal	0.073	0.066	0.112	0.56
Z + jets	0.039	0.017	0.079	1.76
W + jets	0.055	0.087	0.027	1.41
$t\bar{t}$ and Wt	0.018	0.032	0.018	1.03
Single top quark (s-, t-ch.)	0.010	0.018	0.003	0.15
Diboson	0.032	0.040	0.048	0.51
Multi-jet	0.006	0.010	0.005	0.57

STXS measurement (Old scheme)

Latest CMS result

[Phys. Rev. D 109 (2024) 092011]

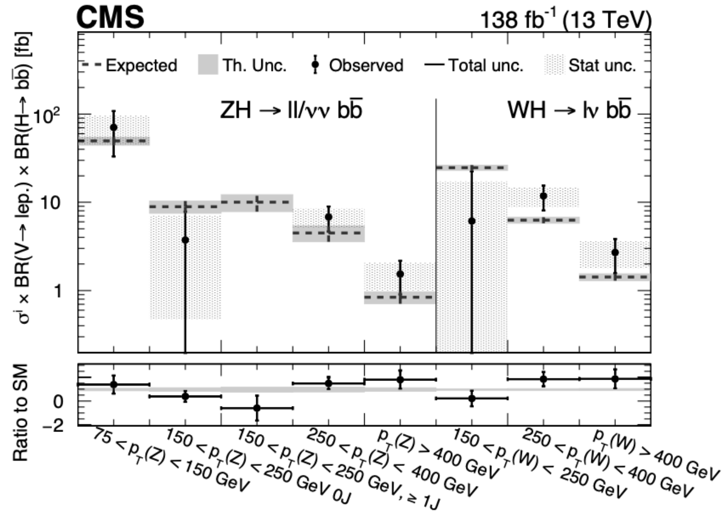

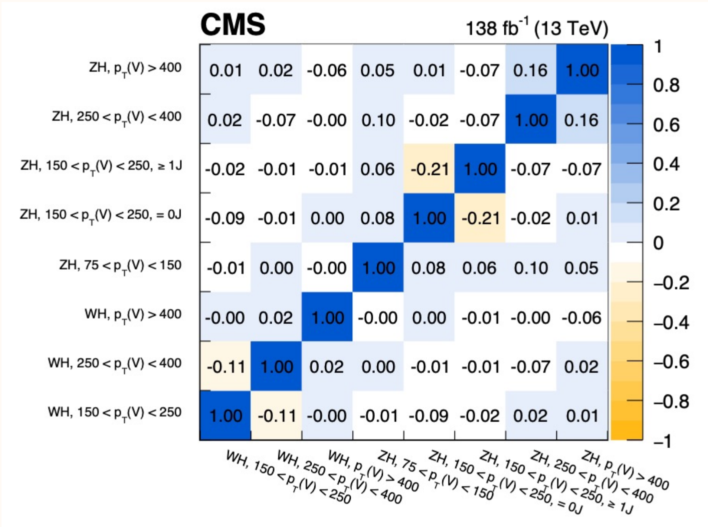
CMS 138 fb^{-1} (13 TeV)

	WH, $150<p_T(V)<250$	WH, $250<p_T(V)<400$	WH, $p_T(V)>400$	ZH, $75<p_T(V)<150$	ZH, $150<p_T(V)<250$, = 0J	ZH, $150<p_T(V)<250$, ≥ 1J	ZH, $250<p_T(V)<400$	ZH, $p_T(V)>400$
ZH, $p_T(V)>400$	0.01	0.02	-0.06	0.05	0.01	-0.07	0.16	1.00
ZH, $250<p_T(V)<400$	0.02	-0.07	-0.00	0.10	-0.02	-0.07	1.00	0.16
ZH, $150<p_T(V)<250$, ≥ 1J	-0.02	-0.01	-0.01	0.06	-0.21	1.00	-0.07	-0.07
ZH, $150<p_T(V)<250$, = 0J	-0.09	-0.01	0.00	0.08	1.00	-0.21	-0.02	0.01
ZH, $75<p_T(V)<150$	-0.01	0.00	-0.00	1.00	0.08	0.06	0.10	0.05
WH, $p_T(V)>400$	-0.00	0.02	1.00	-0.00	0.00	-0.01	-0.00	-0.06
WH, $250<p_T(V)<400$	-0.11	1.00	0.02	0.00	-0.01	-0.01	-0.07	0.02
WH, $150<p_T(V)<250$	1.00	-0.11	-0.00	-0.01	-0.09	-0.02	0.02	0.01

Last ATLAS VHbb resolved+boosted

[ATLAS-CONF-2021-051]

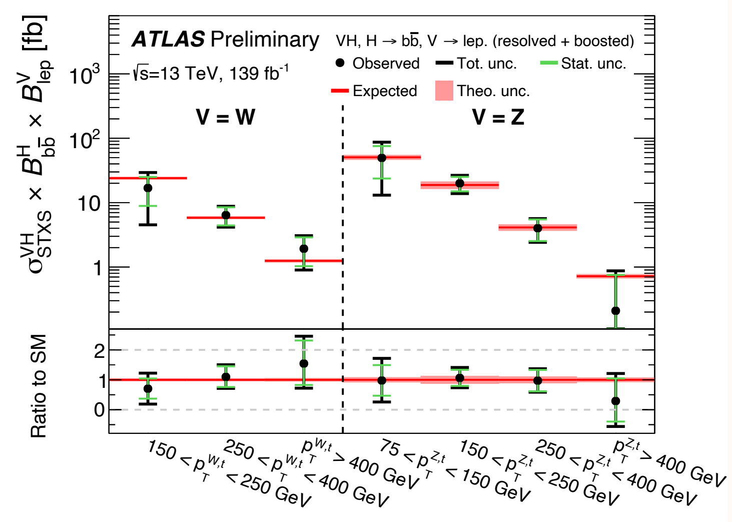

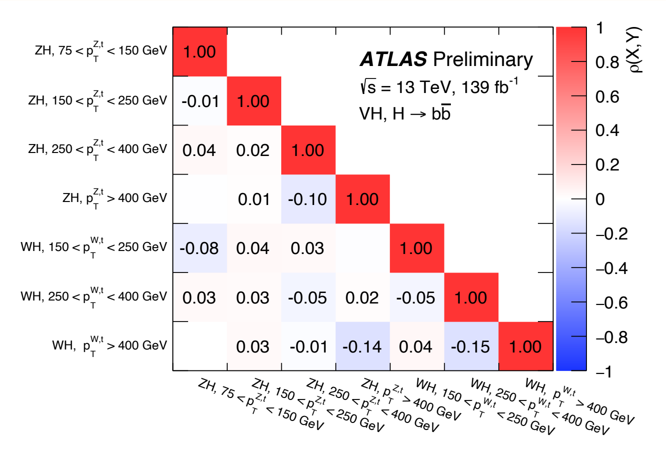
ATLAS Preliminary
√s = 13 TeV, 139 fb^{-1}
VH, H → bb̄

	ZH, $75<p_T^{Z,t}<150$ GeV	ZH, $150<p_T^{Z,t}<250$ GeV	ZH, $250<p_T^{Z,t}<400$ GeV	ZH, $p_T^{Z,t}>400$ GeV	WH, $150<p_T^{W,t}<250$ GeV	WH, $250<p_T^{W,t}<400$ GeV	WH, $p_T^{W,t}>400$ GeV
ZH, $75<p_T^{Z,t}<150$ GeV	1.00						
ZH, $150<p_T^{Z,t}<250$ GeV	-0.01	1.00					
ZH, $250<p_T^{Z,t}<400$ GeV	0.04	0.02	1.00				
ZH, $p_T^{Z,t}>400$ GeV		0.01	-0.10	1.00			
WH, $150<p_T^{W,t}<250$ GeV	-0.08	0.04	0.03		1.00		
WH, $250<p_T^{W,t}<400$ GeV	0.03	0.03	-0.05	0.02	-0.05	1.00	
WH, $p_T^{W,t}>400$ GeV		0.03	-0.01	-0.14	0.04	-0.15	1.00

This analysis

[ATLAS-CONF-2024-010]

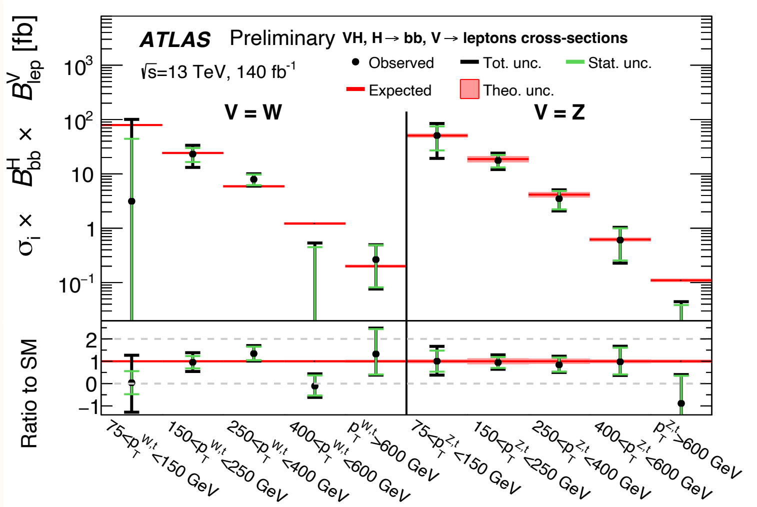

Not published

STXS measurement (New Scheme)

[ATLAS-CONF-2024-010]

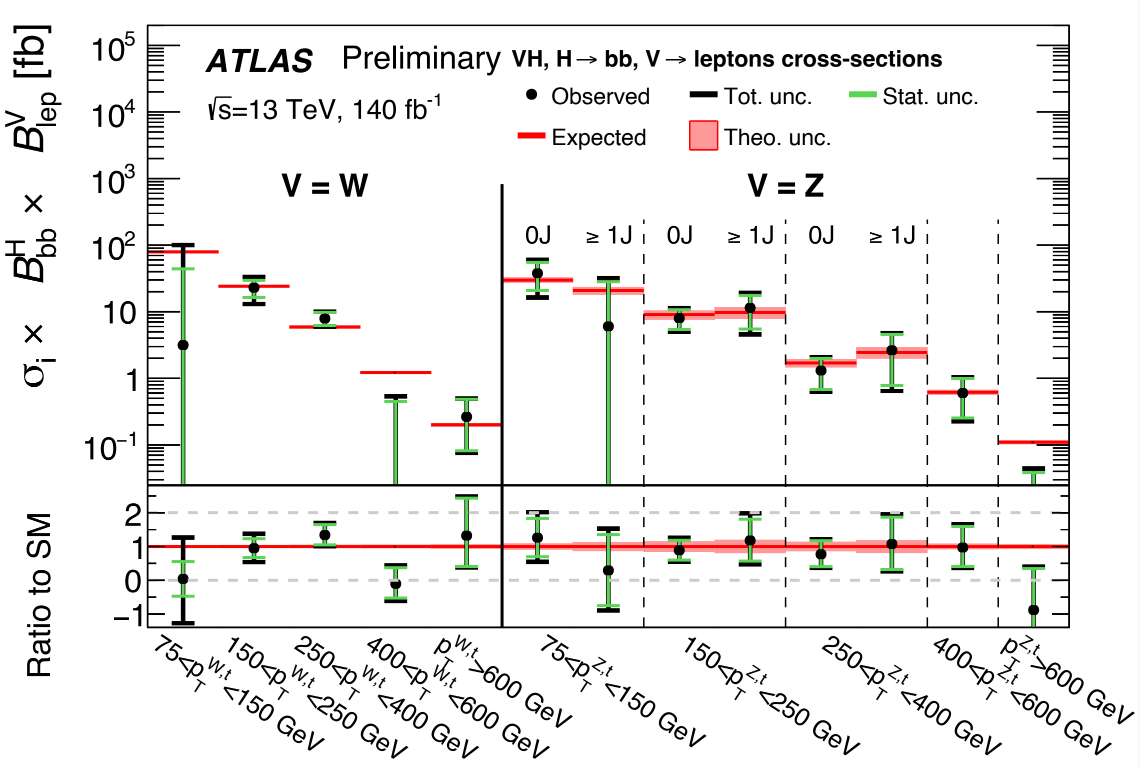

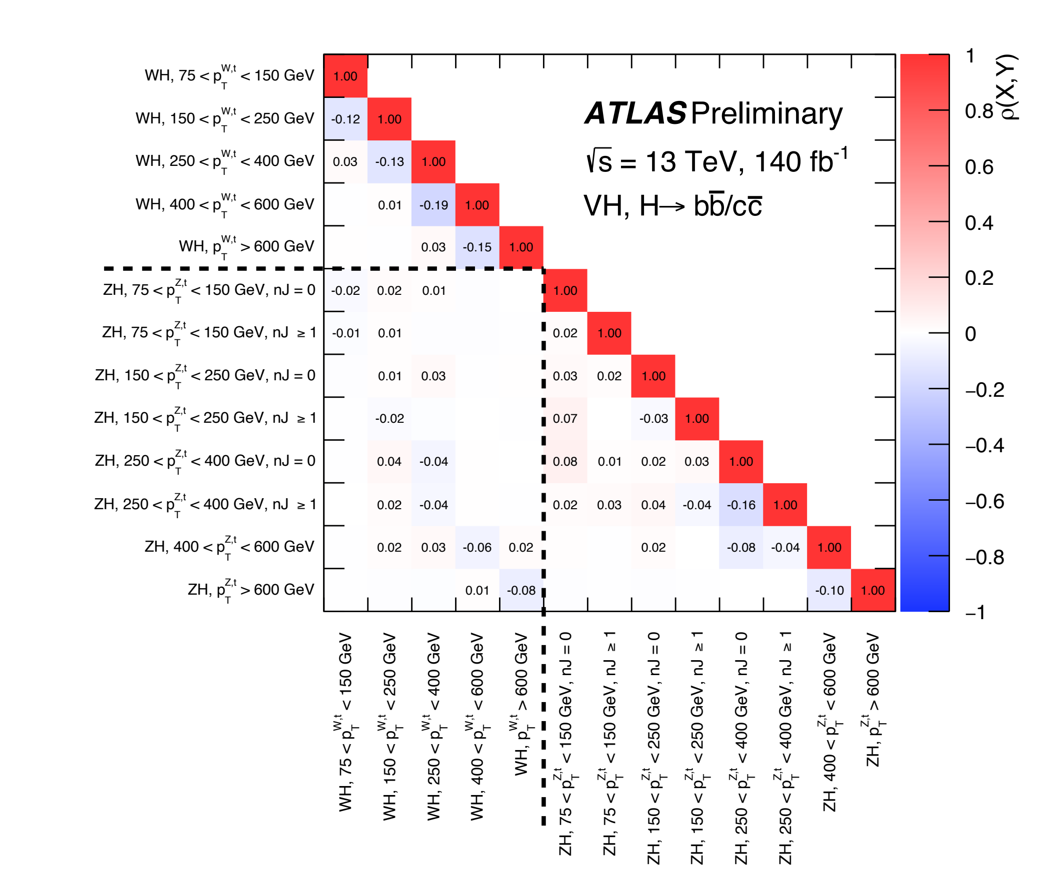

	WH, $75 < p_T^{W,t} < 150$ GeV	WH, $150 < p_T^{W,t} < 250$ GeV	WH, $250 < p_T^{W,t} < 400$ GeV	WH, $400 < p_T^{W,t} < 600$ GeV	WH, $p_T^{W,t} > 600$ GeV	ZH, $75 < p_T^{Z,t} < 150$ GeV, nJ = 0	ZH, $75 < p_T^{Z,t} < 150$ GeV, nJ ≥ 1	ZH, $150 < p_T^{Z,t} < 250$ GeV, nJ = 0	ZH, $150 < p_T^{Z,t} < 250$ GeV, nJ ≥ 1	ZH, $250 < p_T^{Z,t} < 400$ GeV, nJ = 0	ZH, $250 < p_T^{Z,t} < 400$ GeV, nJ ≥ 1	ZH, $400 < p_T^{Z,t} < 600$ GeV	ZH, $p_T^{Z,t} > 600$ GeV
WH, $75 < p_T^{W,t} < 150$ GeV	1.00												
WH, $150 < p_T^{W,t} < 250$ GeV	-0.12	1.00											
WH, $250 < p_T^{W,t} < 400$ GeV	0.03	-0.13	1.00										
WH, $400 < p_T^{W,t} < 600$ GeV		0.01	-0.19	1.00									
WH, $p_T^{W,t} > 600$ GeV			0.03	-0.15	1.00								
ZH, $75 < p_T^{Z,t} < 150$ GeV, nJ = 0	-0.02	0.02	0.01			1.00							
ZH, $75 < p_T^{Z,t} < 150$ GeV, nJ ≥ 1	-0.01	0.01				0.02	1.00						
ZH, $150 < p_T^{Z,t} < 250$ GeV, nJ = 0		0.01	0.03			0.03	0.02	1.00					
ZH, $150 < p_T^{Z,t} < 250$ GeV, nJ ≥ 1		-0.02				0.07		-0.03	1.00				
ZH, $250 < p_T^{Z,t} < 400$ GeV, nJ = 0		0.04	-0.04			0.08	0.01	0.02	0.03	1.00			
ZH, $250 < p_T^{Z,t} < 400$ GeV, nJ ≥ 1		0.02	-0.04			0.02	0.03	0.04	-0.04	-0.16	1.00		
ZH, $400 < p_T^{Z,t} < 600$ GeV		0.02	0.03	-0.06	0.02			0.02		-0.08	-0.04	1.00	
ZH, $p_T^{Z,t} > 600$ GeV				0.01	-0.08							-0.10	1.00

Uncertainties of STXS measurement

STXS region			SM prediction	Measurement	Stat. unc.	Syst. unc. [fb]		
Process	$p_{\mathrm{T}}^{V,\,\mathrm{t}}$ interval	$N_{\mathrm{jet}}^{\mathrm{t}}$	[fb]	[fb]	[fb]	Th. sig.	Th. bkg.	Exp.
$W(\ell\nu)H$	75–150 GeV	≥0	79 .2 ± 2.8	3 ± 100	41	13	88	35
	150–250 GeV	≥0	24.3 ± 1.0	23 ± 10	7	2	7	3
	250–400 GeV	≥0	5.90 ± 0.25	7.9 ± 2.0	1.8	0.5	0.8	0.3
	400–600 GeV	≥0	1.03 ± 0.05	-0.11 ± 0.54	0.46	0.05	0.24	0.09
	> 600 GeV	≥0	0.20 ± 0.01	0.26 ± 0.21	0.20	0.02	0.04	0.03
$Z(\ell\ell/\nu\nu)H$	75–150 GeV	≥0	50.7 ± 3.9	51 ± 32	24	8	19	11
		=0	29.9 ± 2.5	38 ± 22	17	4	12	6
		≥1	20.7 ± 2.6	6 ± 25	25	6	9	8
	150–250 GeV	≥0	18.7 ± 2.3	18 ± 6.0	4.5	2.5	3.0	1.0
		=0	9.0. ± 1.3	8.0 ± 3.2	2.7	0.9	1.4	0.5
		≥1	9.7 ± 1.9	11 ± 7.3	6.0	2.1	3.4	1.5
	250–400 GeV	≥0	4.15 ± 0.45	3.5 ± 1.5	1.3	0.5	0.5	0.2
		=0	1.70 ± 0.22	1.31 ± 0.72	0.65	0.16	0.25	0.10
		≥1	2.45 ± 0.45	2.6 ± 2.1	1.9	0.4	0.7	0.3
	400–600 GeV	≥0	0.62 ± 0.05	0.60 ± 0.40	0.37	0.07	0.12	0.08
	> 600 GeV	≥0	0.11 ± 0.01	-0.10 ± 0.12	0.12	0.01	0.03	0.01

[ATLAS-CONF-2024-010]

Significance of STXS measurement

[ATLAS-CONF-2024-010]

STXS region	post-fit expected	observed
WH, 75 GeV $< p_{\mathrm{T}}^{V,t} <$ 150 GeV	0.7 σ	0.0 σ
WH, 150 GeV $< p_{\mathrm{T}}^{V,t} <$ 250 GeV	2.4 σ	2.3 σ
WH, 250 GeV $< p_{\mathrm{T}}^{V,t} <$ 400 GeV	3.2 σ	4.4 σ
WH, 400 GeV $< p_{\mathrm{T}}^{V,t} <$ 600 GeV	1.6 σ	-0.2 σ
WH, $p_{\mathrm{T}}^{V,t} >$ 600 GeV	1.0 σ	1.5 σ
ZH, 75 GeV $< p_{\mathrm{T}}^{V,t} <$ 150 GeV	1.6 σ	1.6 σ
ZH, 150 GeV $< p_{\mathrm{T}}^{V,t} <$ 250 GeV	3.5 σ	3.4 σ
ZH, 250 GeV $< p_{\mathrm{T}}^{V,t} <$ 400 GeV	3.3 σ	2.7 σ
ZH, 400 GeV $< p_{\mathrm{T}}^{V,t} <$ 600 GeV	1.7 σ	1.7 σ
ZH, $p_{\mathrm{T}}^{V,t} >$ 600 GeV	0.8 σ	-0.7 σ

STXS region	post-fit expected	observed
WH, 75 GeV $< p_{\mathrm{T}}^{V,t} <$ 150 GeV	0.8 σ	0.0 σ
WH, 150 GeV $< p_{\mathrm{T}}^{V,t} <$ 250 GeV	2.4 σ	2.3 σ
WH, 250 GeV $< p_{\mathrm{T}}^{V,t} <$ 400 GeV	3.2 σ	4.4 σ
WH, 400 GeV $< p_{\mathrm{T}}^{V,t} <$ 600 GeV	1.6 σ	-0.2 σ
WH, $p_{\mathrm{T}}^{V,t} >$ 600 GeV	1.0 σ	1.5 σ
ZH, 75 GeV $< p_{\mathrm{T}}^{V,t} <$ 150 GeV, 0 jet	1.4 σ	1.8 σ
ZH, 75 GeV $< p_{\mathrm{T}}^{V,t} <$ 150 GeV, ≥ 1 jet	0.9 σ	0.3 σ
ZH, 150 GeV $< p_{\mathrm{T}}^{V,t} <$ 250 GeV, 0 jet	3.0 σ	2.8 σ
ZH, 150 GeV $< p_{\mathrm{T}}^{V,t} <$ 250 GeV, ≥ 1 jet	1.4 σ	1.7 σ
ZH, 250 GeV $< p_{\mathrm{T}}^{V,t} <$ 400 GeV, 0 jet	2.7 σ	2.0 σ
ZH, 250 GeV $< p_{\mathrm{T}}^{V,t} <$ 400 GeV, ≥ 1 jet	1.3 σ	1.3 σ
ZH, 400 GeV $< p_{\mathrm{T}}^{V,t} <$ 600 GeV	1.7 σ	1.7 σ
ZH, $p_{\mathrm{T}}^{V,t} >$ 600 GeV	0.8 σ	-0.7 σ